Avdelningen för Konstruktionsteknik
Lunds Tekniska Högskola
Box 118
221 00 LUND

Division of Structural Engineering
Faculty of Engineering, LTH
P.O. Box 118
S-221 00 LUND
Sweden

Investigation of cracking due to restraint forces in Swedish concrete slab frame bridges

Utredning om sprickor orsakade av tvångskrafter i svenska betongplattrambroar

Robin Almén

2016

Report TVBK-5252
ISSN 0349-4969
ISRN: LUTVDG/TVBK-16/5252+70p

Engineering degree project
Supervisors: Oskar Larsson, Erik Gottsäter & Thomas Kamrad
May 2016

Abstract

When concrete slab frame bridges are designed with modern linear 3D FE-models large tensile restraint forces will arise in the transversal direction of the bridge from the temperature and shrinkage loads. These restraint forces are much larger than those that are accounted for in the older 2D models. This leads to that the amount of transversal reinforcement, calculated in the 3D FE-calculations, is much higher then what has been standard earlier. This thesis investigated whether or not cracking due to restraint forces is a problem for existing Swedish concrete frame bridges. This was done through modelling existing bridges with 3D FEM. Two different reinforcement models were applied and the calculated amount of reinforcement was compared to the existing reinforcement. Furthermore different types of concrete slab frame bridges were inspected. The different types were bridges with open or closed bottom plate, bridges where the valve was skewed or not and bridges that either crossed a pedestrian/bike path or a car road. Finally the bridges were investigated ocularly to help decide if restraint cracking is a real problem or a problem for the 3D FEM. The results of this investigation showed that cracking was common for bridges that crossed pedestrian/bike paths; however, the crack width was usually within the design limits. Furthermore the results of the comparisons between the two reinforcement models showed that there was a large difference depending on how the restraint forces are accounted for. The standard Eurocode method, where no special regards are taken to the restraint forces, could give an overestimation up to 2000%. The other method, where special regard is taken to the restraint forces, only gave an overestimation up to a maximum of 100%.

Keywords: concrete, slab frame bridges, concrete cracks, cracking, crack control, restraint, restraint forces, finite element.

Sammanfattning

När betongplattrambroar modelleras med moderna linjära 3D FE-modeller kommer stora dragkrafter att uppstå i brons tvärriktning från temperatur- och krympningslasterna. Dessa tvångskrafter är då mycket större än vad som har beaktats i de äldre 2D modellerna. Detta leder till att den tvärgående armeringsmängden, som beräknas i 3D-modellerna, är mycket större än vad som har varit norm innan. Denna avhandling har undersökt huruvida sprickbildning på grund av tvångskrafter är ett problem för befintliga svenska plattrambroar. Detta har gjorts genom att modellera befintliga broar med FEM med olika modeller för att bestämma armeringsbehovet. Därefter har de uträknade armeringsbehoven jämförts med den befintliga inlagda armeringen. Vidare har olika typer av plattrambroar inspekterats. De olika typerna var broar med antingen öppen eller sluten bottenplatta, broar där valvet antingen var skevt eller rak och broar som antingen korsade en gång- och cykelväg eller en bilväg. Slutligen undersöktes broarna okulärt för att avgöra om sprickbildning orsakat av tvångskrafter är ett verkligt problem eller ett problem för 3D FEM. Resultaten av denna undersökning visade att sprickbildning var vanligt för broar som korsade gång- och cykelvägar. Sprickvidderna var däremot vanligtvis inom de tillåtna gränsvärdena. Dessutom visade jämförelserna mellan de två armeringsmodeller att det blev en stor skillnad beroende på hur tvångskrafterna behandlas. Standard Eurokod metoden, där ingen särskild hänsyn tas till de tvångskrafterna, kan ge en överskattning upp till 2000 %. Den andra metoden, där särskild hänsyn tas till tvångskrafterna, gav endast en överskattning upp till max 100 %.

Nyckelord: betong, plattrambroar, betongsprickor, sprickbildning, sprickkontroll, tvång, tvångskrafter, finita element.

Preface

This master thesis is the final product of my studies at the civil engineering program at the Faculty of Technology, Lunds University. The work with the thesis was carried out at the office of Centerlöf & Holmberg AB in Malmö, Sweden under the period of February 2016 to May 2016.

I want to thank my supervisors Erik Gottsäter and Oskar Larsson at the division of Structural Engineering at Lunds Tekniska Högskola and Thomas Kamrad at Centerlöf & Holmberg AB. Without their support and guidance this thesis wouldn't have been possible. I also want thank Mats Persson at Centerlöf & Holmberg for his invaluable assistance with the ocular examination of the bridges. Finally I also want to thank everyone else at Centerlöf & Holmberg for giving me an inspiring place to write my thesis as well as for all the help I got when my supervisors were unavailable.

Malmö, May 2016
Robin Almén

Abbreviations and notations

Abbreviations

2D	**Two D**imensions
3D	**Three D**imensions
BaTMan	**B**ridge **a**nd **T**unnel **Man**agement
CEN	European Committee for Standardization (FR: **C**omité **E**uropeen de **N**ormalization)
EC	**Euro**code
EN	European Standard (DE: **E**uropäische **N**orm)
FE	**F**inite **E**lement
FEA	**F**inite **E**lement **A**nalysis
FEM	**F**inite **E**lement **M**ethod
NA	**N**ational **A**nnex
SS	Swedish Standard (SV: **S**vensk **S**tandard)

Greek upper case letters

ΔT	Change in temperature	$°C$
ΔL	Change in length	m
Δ_{p}	Restraining earth pressure	N/m^2
Δ_{r}	Slip zone	m

Greek lower case letters

α_{cT}	Thermal expansion coefficient for concrete	K^{-1}
α_e	Ratio of steel/concrete modulus's of elasticity	-
β	Angle of slope	°
γ	Weight	N/m^3
δ	Deformation | Angle between principal moment and reinforcement	m | °
δ_σ	Deformation, stress-dependent	m
δ_T	Deformation, stress-independent (Thermal)	m
δ_{tot}	Deformation, total	m
ε	Strain	$-$
$\varepsilon_{\sigma,rest}$	Strain, fictive stress-dependent from restraint loads	$-$
ε_{cT}	Strain, thermal strain for concrete	$-$
ε_s	Strain, steel	$-$
$\varepsilon_{sm} - \varepsilon_{cm}$	Differential strain between concrete and reinforcement	$-$
ρ	Reinforcement ratio	$-$
ρ_{eff}	Reinforcement ratio, effective	$-$
ϕ	Diameter of reinforcement bars	m
ϕ_d	Design friction angle	°
φ	Creep coefficient	$-$
σ	Stress	Pa
σ_c	Stress, concrete	Pa
σ_s	Stress, steel	Pa
$\sigma_{s,add}$	Stress, additional steel	Pa
σ_{ep}	Vertical earth pressure	Pa
ψ	Angle between principal moment and deformation	°

Latin upper case letters

A_c	Concrete area	m^2
$A_{c,eff}$	Concrete area, effective area	m^2
A_{ct}	Concrete area , tensile zone prior to cracking	m^2
A_s	Reinforcement area	m^2
$A_{s,min}$	Reinforcement area, minimum	m^2
E_c	Modulus of elasticity for concrete	Pa
E_{cm}	Modulus of elasticity for concrete, mean value	Pa
$E_{c,eff}$	Modulus of elasticity for concrete, effective value	Pa
E_s	Modulus of elasticity for reinforcement	Pa
F	External force	N
H	Height of an element	m
K_0	Lateral earth pressure coefficient at rest	$-$
K_0^*	Lateral earth pressure coefficient at rest with a slope	$-$
L	Length of an element	m
M_1 / M_2	Moment, principal direction	Nm
M_x / M_y	Moment, reinforcement direction	Nm
N	Normal force	N
$N_{c,rest}$	Normal force, restraint force in concrete	N
N_{ext}	Normal force, external force	N
T	Temperature	K
T_N	Temperature, even distributed thermal component	K
T_M	Temperature, vertical linear temperature difference	K

Latin lower case letters

c	Concrete cover | cohesion constant	$m \mid N/m^2$
f_{ck}	Concrete compression strength, characteristic value	Pa
f_{ctm}	Concrete tensile strength, mean value	Pa
$f_{ct,eff}$	Concrete tensile strength, mean value at time of cracking	Pa
f_{yd}	Steel tensile strength	Pa
g_{pav}	Permanent load, pavement	N/m^2
g_{ep}	Permanent load, earth pressure	N/m^2
k	Coefficient, regards the non-uniform self-equilibrating stress	$-$
k_1	Coefficient, regards the bond properties of reinforcement	$-$
k_2	Coefficient, regards the strain distribution	$-$
k_3	Constant given in the Swedish NA	$-$
k_4	Constant given in the Swedish NA	$-$
k_c	Coefficient, regards the stress distribution prior cracking	$-$
k_t	Coefficient, regards the duration of the load	$-$
l_t	Bond stress transfer length	m
$s_{r,max}$	Maximum crack spacing	m
t	Time	h
w_k	Crack width, characteristic value	m
w_{max}	Crack width, maximum value	m
z	Depth of the soil	m

Table of Contents

1. Introduction

1.1. Background

When concrete slab frame bridges are designed with linear 3D FE-models consideration must be made to regard for effects of thermal loads and shrinkage. These loads will force the concrete elements in the bridge to retract, which the elements are unable to do due to the nature of the geometry of the slab frame bridge. For a linear FEA with design values on thermal and shrinkage loads this will give rise to very large restraint forces which in turn will lead to a large amount of reinforcement being prescribed to limit the crack width. The amount of calculated reinforcement will then be much higher then have been standard prior to the implementation of 3D FEA in the industry. This has become a large problem for the industry since the load cases defined in the Eurocodes are not suited for these types of FE-analyses. In addition the Swedish Transport Administration is also demanding FEA for all new bridge constructions.

The reason for the errors of the FE-models is that the magnitude of restraint forces is depending on the stiffness of the deforming element. For a linear FEA the stiffness of concrete is assumed to be constant where as in reality the stiffness is reduced, and so the restraint forces, when the concrete cracks (Engström, 2014, s. 108). Since making a non-linear analysis of slab frame bridges is often too time consuming, other ways must be employed to take the non-linearity of concrete in a linear analysis into account. This behaviour as well as different analyse methods has already been studied by for example (Alfredsson & Spåls, 2008), (Andersson & Andersson, 2010), (Kamali, Johansson, & Svedholm, 2013) and (Ledin & Christensson, 2015). However these studies have been limited in coverage and not validated by field tests.

This thesis will continue on the works above and try to evaluate whether or not cracks caused by restraint forces are common for Swedish slab frame bridges as well as try to determine the correctness of some of the proposed calculation methods.

1.2. Aim

In general, the aim of this thesis is to determine whether or not cracks due to restraint loading are a real problem for Swedish concrete slab frame bridges.

To do this the following three issues are to be determined.

1. Establish whether or not cracks caused by restraint forces are common for Swedish concrete slab bridges.
2. Establish which geometrical properties cracked bridges respective non-cracked bridges have in common.
3. Evaluate different reinforcement models which determine the amount of reinforcement needed for concrete slab bridges with FEA.

1.3. Method

First a literature study was carried out where restraint forces, the cracking process and ways to determine the source of concrete cracks were studied.

Following that an investigation of Swedish concrete slab bridges was made. The investigation started with an analysis of the Swedish Transport Administrations (sv: Trafikverkets) bridge and tunnel database BaTMan. There technical drawings were collected for chosen bridges. After that FE-analysis's were made on the chosen bridges to determine the amount of reinforcement required for

crack width limitation according to two different models. The results were compared to the actual reinforcement amount in the bridges.

Finally excursions were carried out to the chosen bridges. The bridges were examined for whether or nor not they had cracked. If they had cracked then data on the amount and width of the cracks were collected. The cracking was then compared to the results of the FEA for every bridge.

Thereafter all the results are compared in order to answer the issues asked in 1.2.

1.4. Limitations

There is a phenomenon that causes restraint forces and cracking but which is not discussed in this thesis namely early thermal contraction. Early thermal contraction is caused by an excessive heat generation during the concrete hardening process. The reason why this phenomenon is not considered in this thesis is that it's a production problem and not a design problem. This means that cracking due to early thermal contraction is caused by an insufficient counter measure during the production and not due to design errors. Cracks caused by early thermal contractions are most often mended during the production phase (Kamrad, 2016).

The thesis will only consider single span concrete frame bridges as those types are the most common of the frame bridges. (Kamrad, 2016).

1.5. Outline of the thesis

The report is divided in four major chapters.

The first chapter, chapter 2, gives the theoretical background for the thesis. The chapter starts by describing the design of a concrete slab frame bridge and the different types of phenomenon that can cause cracking in concrete. Furthermore the phenomenon known as stress-independent strain is explained and how it's related to restraint forces. Following that the cracking process is explained for different types restrained elements affected by stress-independent strains. Finally the design rules for crack control are presented for the different reinforcement models which are to be investigated.

The entire investigation process is then explained in chapter 3. First the bridge selection process from BaTMan is described. Following that the finite element analysis is thoroughly explained for two of the 11 investigated bridges. Finally an explanation of the methods of ocular bridge inspection is presented.

The results are then presented in chapter 4. Here the full results of the investigation are shown only for the two bridges above; the rest are available in the first appendix. In the end of the chapter there are two summarized tables with some of the results for all the bridges.

Finally the conclusions of the thesis along with sources of errors and further research ideas are are discussed in chapter 5.

2. Theory – Concrete slab frame bridges, restraint forces and cracking

2.1. General

Concrete slab frame bridges are a common bridge type for smaller bridge spans. One of their major problems is that they are statically undetermined which means that they will suffer from restraint forces. Restraint forces arise when a restraint element is affected by a stress-independent strain. The prevented deformation will then give rise to large tensile stresses which will cause concrete elements to crack. To handle this slab frame bridges are designed in the serviceability limit state for a certain crack width depending on the exposure class, concrete quality and life span.

2.2. Concrete slab frame bridges

In Sweden, slab bridges and beam bridges are the most common bridge types, of which the slab frame bridge is the most common. Different types of slab frame bridges exist and some of them are shown in Figure 1 (Sundquist, 2009, s. 21).

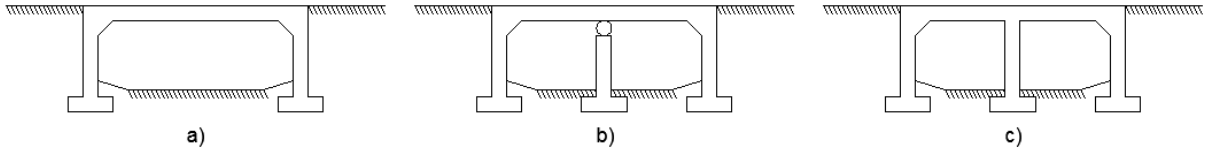

Figure 1 – Slab frame bridges
a) single span, b) multiple spans with pier support, c) multiple spans with full frame support (Sundquist, 2009, s. 22).

Slab frame bridges are used for spans up to of 20-25 m. A larger span can be used but then pre-stressed reinforcement must be used or the thickness of the slab must be increased beyond economical limit (Sundquist, 2009, s. 23). Furthermore the shape of a slab frame bridge can vary where a common variation is the shape of the bottom plate. The bottom plate can either be a single large slab which is called a closed bottom plate, or two separate foundations which are called an open bottom plate. A sketch of a slab frame bridge with a closed bottom plate can be seen in Figure 2.

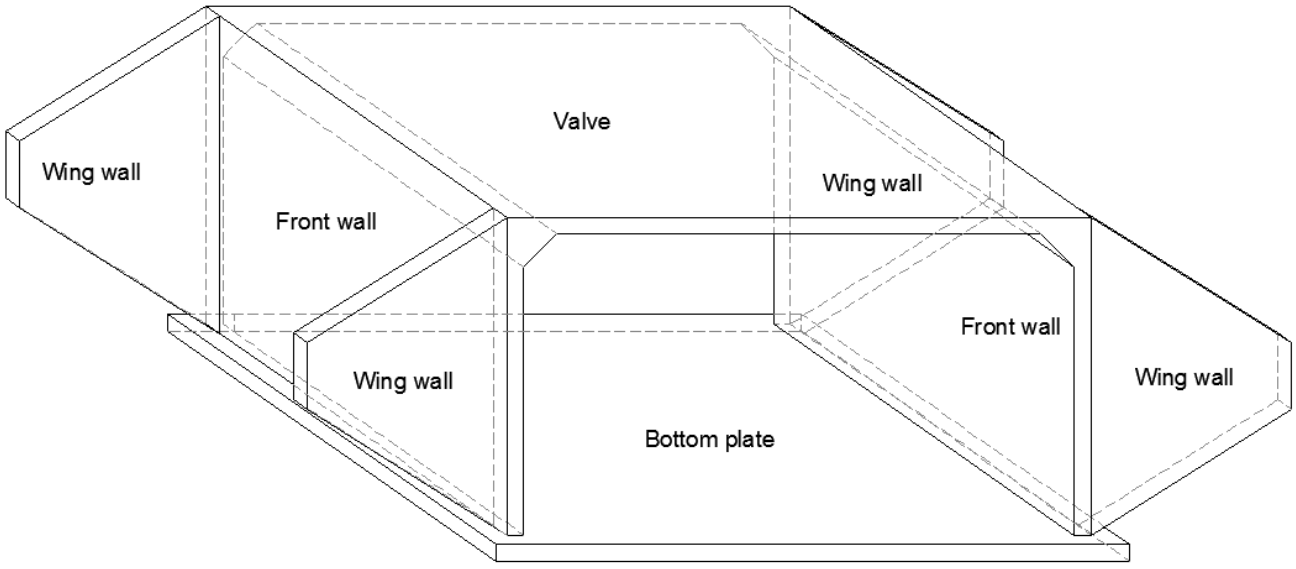

Figure 2 – Schematic picture of a slab frame bridge with wing walls on a closed bottom plate.

Concrete frame bridges are usually cast in two steps. First the bottom plate is cast and a few weeks later the rest of the superstructure is cast. If the bridge is wider then 15-18 m then the superstructure can be cast in more phases. (Kamrad, 2016)

The benefits of having a frame are many. Horizontal forces are dealt with by the frame effect, meaning that the rigid corner will lead the horizontal force down vertically into the ground. Additionally the maximum moment of the slab is lower than if the slab had been simply supported. The cost is also lower for both production and maintenance since no bearings or expansion joints have to be included. The disadvantages are however that the slab is statically undetermined which means that restraint forces will arise (Sundquist, 2009, s. 24).

2.3. Crack assessment

The main reasons the width of the cracks should be limited are according to (Ghali & Favre, 1994, ss. 343-344) and (The Concrete Society, 1992, s. 14) the following:

- Maintain good aesthetic appearance
- Maintain durability, i.e. limit the risk of corrosion for the reinforcement
- Maintain the tightness of the concrete.
- Maintain structural load capacity

It's hard to define a certain crack width where good aesthetic appearance can be said to be impaired, since aesthetic values is very subjective. If only aesthetic is to be regarded cracks up to 0.3 mm are generally accepted; but for more prestigious structures crack acceptance could be low as 0.1 mm whereas for very seldom used structures cracks up to 0.7 mm could be accepted (The Concrete Society, 1992, ss. 14-15).

The risk for reinforcement corrosion is highly dependent on the geometry of the cracks compared to the geometry of reinforcement. Cracks can either be parallel and coincident with the reinforcement or perpendicular and intersecting to the reinforcement. For cracks that are coincident there is always a risk for corrosion independent of the crack width, whereas for the intersecting crack the risk for corrosion increases with the number of cracks and not the cracking width (The Concrete Society, 1992, s. 16).

When water enters a concrete crack a phenomenon known as "autogenous healing" can occur. This healing effect is the result when the water dissolves calcium hydroxide from the concrete which can then react with the carbon dioxide in the air and form solid crystals of calcium carbonate. If the crack is sufficiently small, 0.2 mm or lower, the crack can close itself within a week (The Concrete Society, 1992, ss. 14-15).

As this thesis focuses on the service state of bridges the effects cracking has on the structural capacity is not investigated.

To be able to identify cracks caused by restraint forces it's vital to be able to distinguish them from cracks caused by other causes. A number of non-structural cracks are listed in Figure 3 and the most common of these are shortly explained in Table 1.

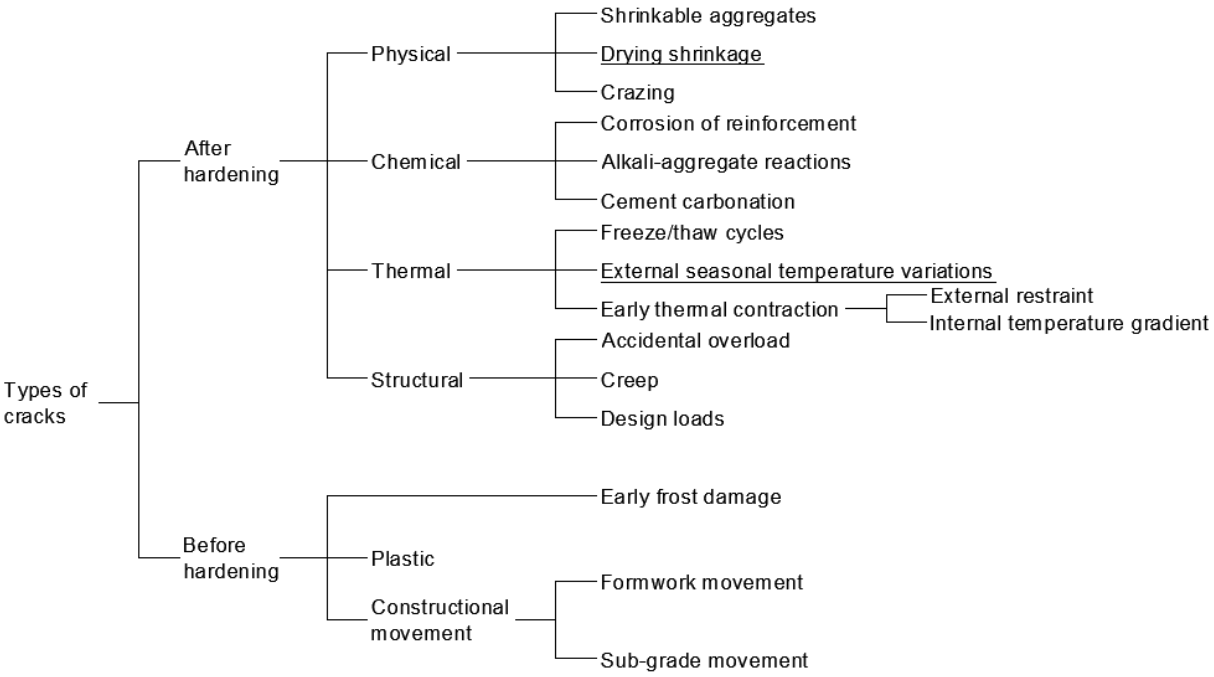

Figure 3 – Table of cracks with investigated cracks underlined (The Concrete Society, 1992, s. 9)

Table 1 – Classification of the most common concrete cracks. (Table rewritten from (The Concrete Society, 1992, s. 10))

Type of cracking	Subdivision	Most common location	Primary cause (excluding restraint	Secondary cause / factors	Remedy (assuming redesign is impossible)	Time of appearance
Plastic settlement	Over reinforced	Deep sections	Excess bleeding	Rapid Early drying conditions	Reduce bleeding (air entrainment or revibrate)	Ten minutes to three hours
	Arching	Top of columns				
	Change of depth	Trough and waffle slabs				
Plastic shrinkage	Diagonal	Roads and slabs	Rapid early drying	Low rate of bleeding	Improve early curling	Thirty minutes to six hours
	Random	Reinforced concrete slab				
	Over reinforced	Reinforced concrete slab	Ditto plus steel near surface			
Early thermal contraction	External restraint	Thick walls	Excess heat generation	Rapid cooling	Reduce heat and / or insulate	One day to two or three weeks
	Internal restraint	Thick slabs	Excess temperature gradient			
Long-term drying shrinkage	-	Thin slabs and walls	Inefficient joints	Excess shrinkage, inefficient curing	Reduce water content, improve curing	Several weeks or months
Crazing	Against formwork	'Fair faced' concrete	Impermeable formwork	Rich mixes, poor curing	Improve curing and finishing	One to seven days, sometimes much later
	Floated concrete	Slabs	Over-trowelling			
Corrosion of reinforcement	Natural	Columns and beams	Lack of cover	Poor quality concrete	Eliminate causes listed	More than two years
	Calcium chloride	Precast concrete	Excess calcium chloride			
Alkali-silica reaction	-	Damp locations	Reactive aggregate plus high alkali cement		Eliminate causes listed	More than five years

2.4. Stress-independent strains

When calculations are to be made regarding deformation of concrete it is imperative to know whether the strain is stress-dependent or stress-independent.

Stress-dependent strains are caused by external forces acting on the structure, causing deformations. The forces can be caused either by an initial load like self-weight, soil pressure and traffic load, or by a time dependent load like creep (Engström, 2014, ss. 15-16).

Stress-independent strains are on the other hand caused by phenomenon that causes a deformation and not a stress, such as thermal concrete strain or shrinkage of concrete. Here the magnitude of the stress is dependent on the prevented deformation (Engström, 2014, ss. 15-16).

2.4.1. Thermal concrete strain

When the temperature of a material changes thermal strain will appear and results in a change of volume. This is true for all forms of materials (Jönsson, 2010, s. 19).

For bridges it is reasonable to assume that the temperature is constant across the length but varying across the cross section. Different factors influence the temperature distribution of a cross section such as its geometry, thermal parameters, and the local weather (Ghali & Favre, 1994, ss. 297-298). For example on a cold winter night the surface of the valve would become colder than the bottom of the

bottom plate due to the temperature variance in the concrete. This would lead to uneven temperature contraction where the valve wants to contract more than the front walls it's connected to.

The thermal strain for concrete can be calculated by Equation (2.1) (Jönsson, 2010, s. 19), which can be rewritten into Equation (2.2):

$$\frac{\Delta L}{\mathrm{L}} = \alpha_{cT} \cdot \Delta T \tag{2.1}$$

$$\varepsilon_{cT} = \alpha_{cT} \cdot \Delta T \tag{2.2}$$

where

L	Is the initial length of the element
$\Delta\mathrm{L}$	Is the change of length of the element
α_{cT}	Is the thermal expansion coefficient for concrete
$\Delta\mathrm{T}$	Is the change of temperature in the element
ε_{cT}	Is the thermal strain for concrete

The thermal expansion coefficient for concrete is highly dependent on the type of cement and aggregate. For concrete where the aggregate consists mainly of granite the coefficient is around $9 \cdot 10^{-6}\ K^{-1}$, whereas aggregate consisting of quartzite has a coefficient of $13 \cdot 10^{-6}\ K^{-1}$ (Engström, 2014). If the aggregate material is not known a value of $10 \cdot 10^{-6}$ for the thermal expansion coefficient may be chosen (SS-EN 1992-1-1, 2005, s. 26).

2.4.2. Shrinkage of concrete

The shrinkage strain of concrete depends mostly on the relative humidity of the location. Shrinkage strain starts to develop during the hardening process and continue forever but with diminishing speed. The total shrinkage strain consists of two parts, drying shrinkage and autogenous shrinkage (Engström, 2014, s. 131).

Drying shrinkage is the volume change effect from the exchange of moisture between the concrete and its surroundings. The effect of drying shrinkage is mostly dependent on the water-cement ratio and permeability of the concrete and the relative humidity of the surroundings (Engström, 2014, ss. 131-132).

Autogenous shrinkage is due to the volume decrease of the late hydration inside the concrete. A hardened concrete will often possess some cement that hasn't reacted yet but will continue to react with the natural moisture inside the concrete. This in turn will lead to a volume decrease which is the autogenous shrinkage (Engström, 2014, s. 138).

Uneven shrinkage occurs when a new concrete part is cast onto an existing part. For concrete bridges the bottom plate is usually cast before the superstructure. As the shrinking speed is decreasing with time the bottom plate will restrain the superstructure from shrinking at full speed (Engström, 2014, ss. 18-19).

2.5. Restraint forces and restraints

Restraint forces occur when a structural element is exposed to stress-independent strain but is unable to deform due to the nature of its boundary condition. To achieve equilibrium a restraint force corresponding to the prevented displacement will appear, see Figure 4 for an example (Engström, 2014, s. 8).

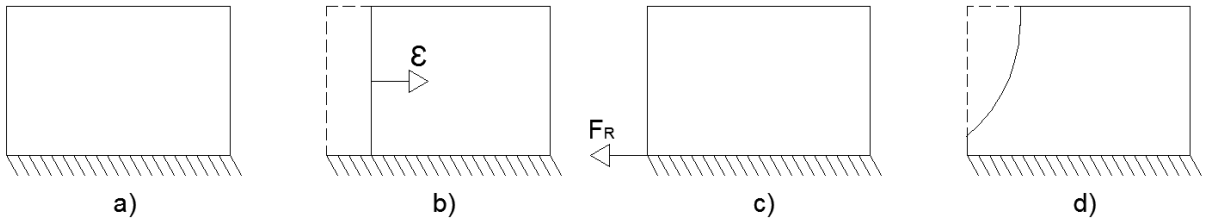

Figure 4 – General behaviour of restraint forces
a) Restrained wall, b) uniformed strain ε applied with no regards taken to restraint, c) restraint force F_R appears and "pull back" the wall to its original position d) The final deformed state, note that there is no restraint force at the top of the wall which enable the wall to deform above the ground as there are no or low restraint forces there.

These stress-independent strains will give rise to tensile or compressive stresses, through the restraint forces, in restrained elements.

Since the restraint force should correspond to the prevented displacement, the stiffer an element is the larger the restraint force is for the same prevented displacement. A consequence of this is that when the stiffness decreases through e.g. cracking, so does the restraint force (Engström, 2014, s. 23), (Kamali, Johansson, & Svedholm, 2013).

There are two types of restraints that give restraint forces, external and internal restraints. External restraints are when the structure is prevented to from deforming because of its boundary condition. (Engström, 2014, ss. 23-24). An internal restraint occurs when different parts of a cross section have different stress-independent strains. These different parts of the cross-section will then prevent the other parts to deform fully and cause restraint forces, known as "eigenstresses" since they must cancel each other out to achieve equilibrium (Engström, 2014, s. 28).

2.5.1. Example of external restraints

Bellow follows two theoretical examples of external restraints. First is a concrete wall that is restrained to the floor and subjected to shrinking, Figure 5 (a). This restraint type is called an edge restraint, since the wall is restrained along one of its edges. As the floor is preventing the wall to shrink in the longitudinal direction tensile stresses will develop along the boundary. If the tensile stresses surpass the tensile strength of the concrete, cracking will occur, Figure 3 (b). After cracking the element is still restrained and will continue to crack, Figure 5 (c) (Engström, 2014, ss. 97-98).

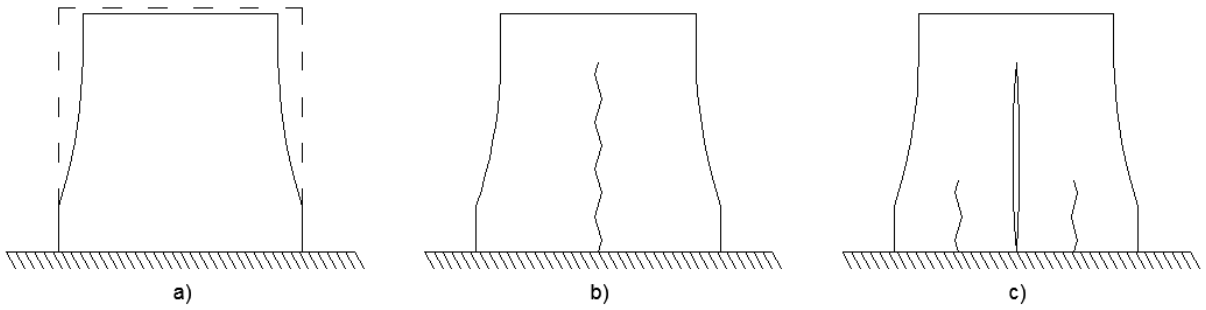

Figure 5 – Concrete wall cracking
a) shrinking before cracking, b) first crack development, c) more cracks appear and first crack expand due to continued shrinkage. (Engström, 2014, s. 97).

In another example of a restraint situation, a concrete beam is restrained between two walls and also subjected to shrinking, Figure 6 (a). This restraint type is called an end restraint. As the beam is completely restrained in two edges tensile stresses will develop from the restraint forces. If the tensile stresses surpasses the tensile strength of the concrete the beam will crack and split into two parts,

Figure 6 (b). As the element is no longer restrained in both edges the restraint force will disappear and the element will deform accordingly, Figure 6 (c) (Engström, 2014, s. 97).

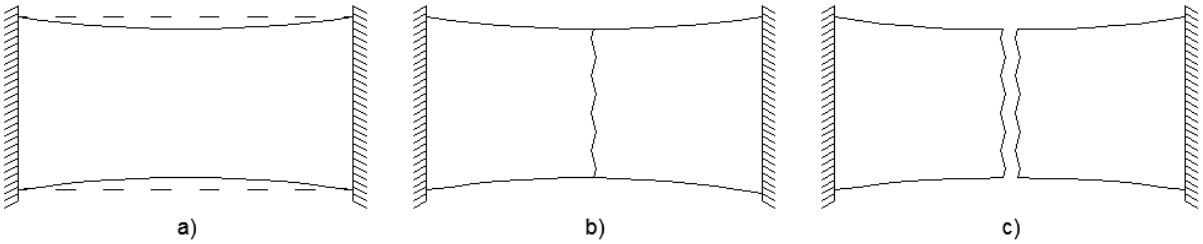

Figure 6 – Concrete beam cracking
a) shrinking before cracking, b) crack development, c) element split into two parts and free to shrink longitudinally. (Engström, 2014, s. 97).

From a real design perspective it is quite common for slab frame bridges to have different temperatures in the front walls compared to the valve. This can lead to that the front wall will restrain the valve from shrinking, with the effect of Figure 6 above.

2.5.2. Example of internal restraints

Below follows three different examples of internal restraints. First is a reinforced concrete beam shown in Figure 7, which is subjected to uniform shrinkage.

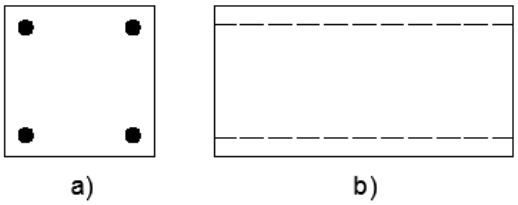

Figure 7 – Reinforced concrete beam.

As the reinforcement does not shrink it will not develop shrinkage strain and thus act as a partial restraint to the shrinking concrete. This means that the shrinkage of concrete will apply a stress-dependent compression strain on the reinforcement and that the reinforcement will apply a stress-dependent tensile strain on the concrete (Engström, 2014, ss. 28-29).

To demonstrate this behaviour Figure 8 is used. Figure 8 (a) shows the reinforced concrete beam unaffected by shrinkage. Assuming that the concrete and reinforcement acts independently of one another, the concrete can shrink freely, this is shown in (b). Then a theoretical force is placed on the reinforcement, compressing it to the same length as the concrete, se (c). At last, it is assumed that the concrete and reinforcement act dependently and the compression force acting on the reinforcement is removed. The reinforcement will now try to expand back to its original position (a) and the concrete will try to revert back to position (b). A position as in Figure 8 (d) will then be reached as the stresses from the deformations reaches equilibrium (Engström, 2014, ss. 29-30).

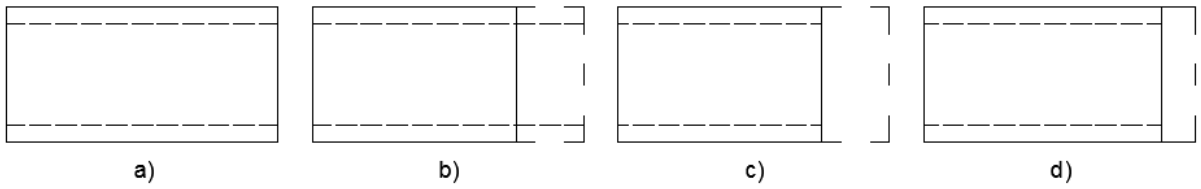

Figure 8 Reinforced concrete beam
a) unaffected by shrinkage, b) independent shrinkage of concrete, c) compression of reinforcement, d) Equilibrium.

A second example of internal restraint is a concrete element being cast on a previously cast element. The two different concrete elements will have different needs of shrinkage, as the older element already has shrunk a bit. The same method as above can be used, i.e. one element assumes to shrink while the other element is affected by the theoretical compression force (Engström, 2014, ss. 34-35).

Furthermore a concrete element can be affected by a non-linear stress-independent strain distribution. This means that the element itself is preventing it from deforming freely. An example of this is a concrete element where the outer parts are drying quicker than the inner parts. This will lead to an uneven shrinkage strain distribution, where the inner part of the element is preventing the outer part from deforming freely. This in turn leads to tensile stresses in the outer part of the element and compressive stresses in the centre part of the element. Another example of uneven strain distribution is a concrete deck being cooled by rain. The outer parts of the deck will then cool down quicker than the inner parts. This means that internal restraint forces can arise even though an element is permitted to deform due to both internal and external boundary conditions. An example can be an element which has a local temperature variation. (Engström, 2014, s. 34).

2.6. Restraint degree

The restraint degree is a value which indicates how much of the desired deformation due to restraint effects is prevented. It can vary between 0 and 1, where 0 means that the deformation is not prevented at all and 1 means that the deformation is fully prevented.

For an edge restrained element shrinking in the longitudinal direction, the restraint degree decreases further away from the restraint. Furthermore the restraint degree is highly depended on the ration between the length and height of the element (Engström, 2014, ss. 37-38), see Figure 9 and 10.

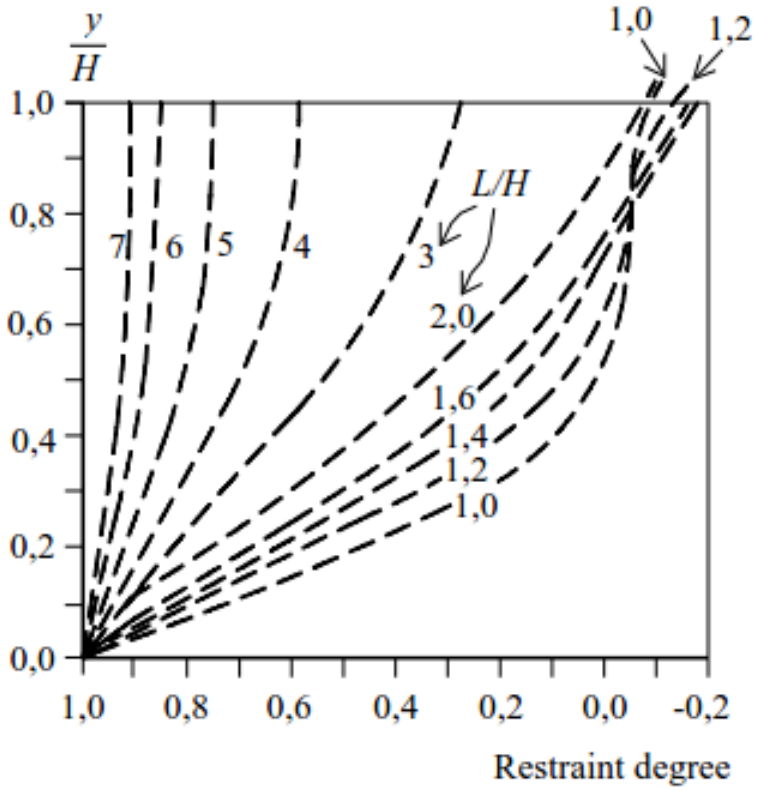

Figure 9 – Restraint degree as a function of L/H (Engström, 2014, s. 38).

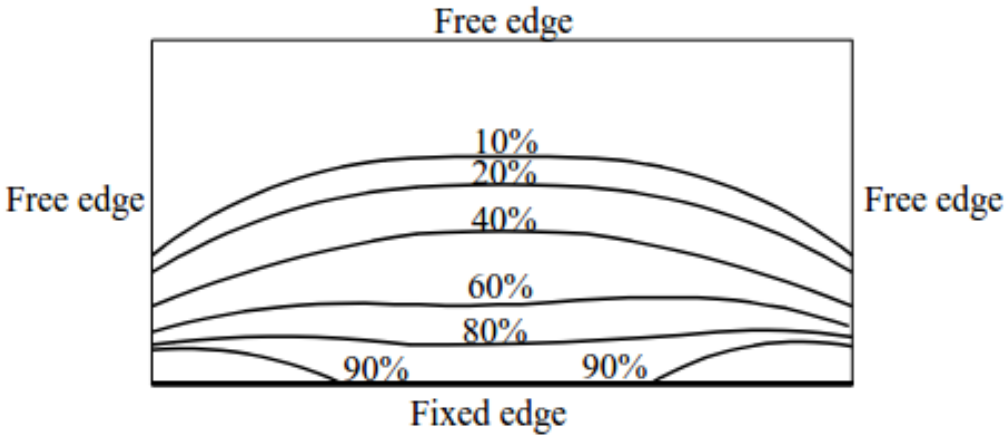

Figure 10 – Restraint degree (as percentage) varying inside a one side restraint element (Engström, 2014, s. 38).

2.7. Cracking process from restraint forces

The cracking process differs between different types of concrete element depending on their boundary condition, loading condition and reinforcement.

Below follow four different examples of cracking depending on the restraint type.

2.7.1. Non-reinforced element – two edge restraint

As shown in Figure 6, cracking in a two edge restrained element is due to tensile stresses arising in the longitudinal direction of the element. If these stresses supersede the tensile strength of the element the

crack will cut the element in two, which will then be able to deform longitudinally (Engström, 2014, s. 97).

2.7.2. Non-reinforced element – one side restraint

As shown in Figure 5 the cracking of a one side restrained element is due to tensile stresses arising along the restraint. If these stresses supersedes the tensile strength of the element cracks will appear, but the element will still be restrained. This leads to, unless the strain decreases, more cracks appearing between the earlier cracks as well as a widening of earlier cracks (Engström, 2014, ss. 97-98).

It has been found by Alfredsson & Spåls (2008, s. 94) that the cracks appear in arch like bands, shown in Figure 11. It was theorised that when the principal stress reached the tensile capacity, a crack was created between the arch and the middle of the restrained side. After a crack had appeared, new arches were created either between the unrestrained sides and a crack or between two cracks. Their study showed that cracks close to the short edges could appear inclined and perpendicular to the arches, whereas the cracks close to the middle were almost always vertical. The arches are demonstrated in Figure 11.

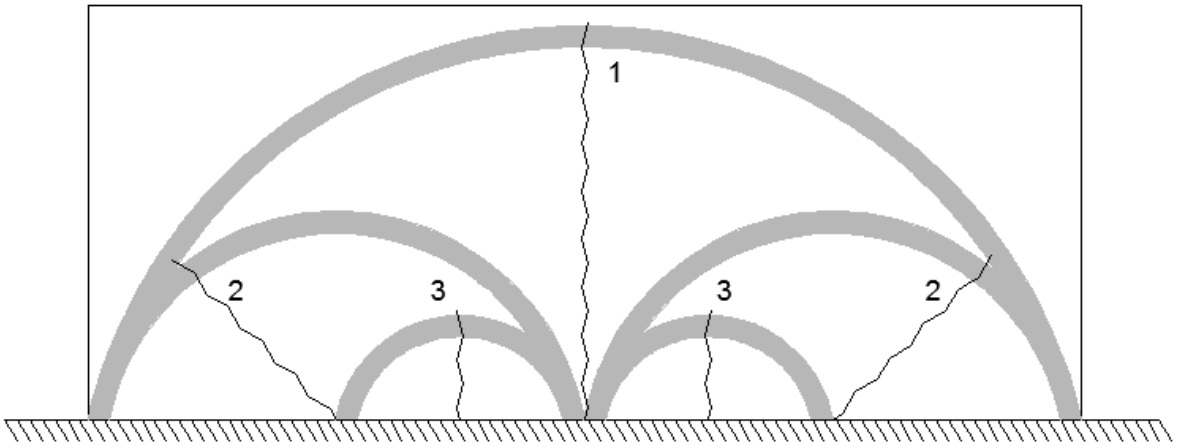

Figure 11 – Possible cracking behaviour discovered by Alfredsson & Spåls. The numbers represent the order in which the cracks appear (Engström, 2014, s. 98).

2.7.3. Thin reinforced bar

When a reinforced concrete bar is loaded by tensile forces in the reinforcement, the stress in the reinforcement will transfer over to the concrete over a distance l_t due to shear stress called bond stress. This means that over the distance l_t the tensile stress in the steel decreases as the tensile stress in the concrete increases. At the ends of the bar the bond stress causes local concrete failure, so called slip, in the zone Δ_r as the bond stress supersedes the shear strength (Engström, 2014, ss. 99-100). Se Figure 12 for a graphical explanation of the stresses in a reinforced concrete element.

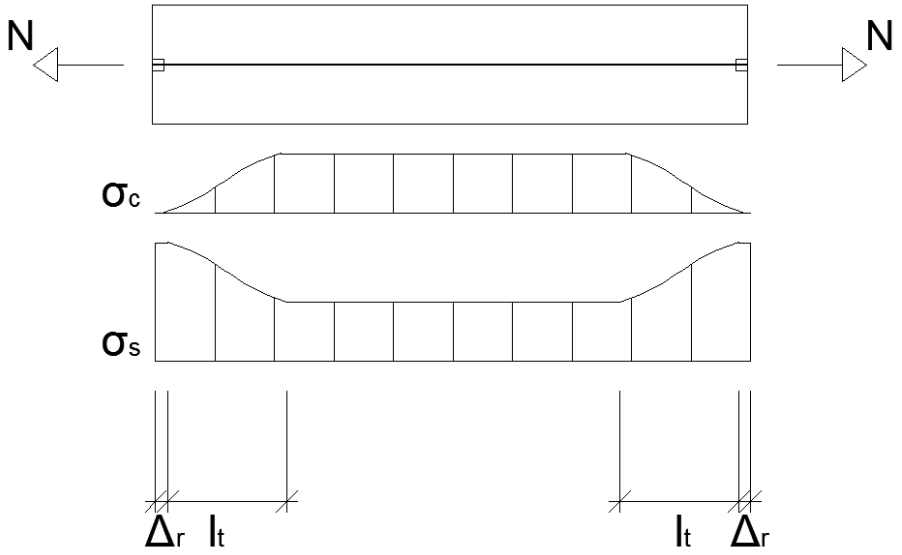

Figure 12 – Stress distribution for a reinforced concrete element (Engström, 2014, s. 99).

If the tensile force N increases and the concrete stress σ_c equals or supersedes the tensile strength, the concrete will crack which leads to that the bar will be split into two parts. The two parts will then behave the same way as before, meaning that there will be a slip at the two edges of the crack and that the concrete stress will decrease and increase after the crack. If the zone between the crack and the free edge (or another crack) is lower then $2l_t$ then there is no risk for another crack to appear as the concrete stress will not achieve the magnitude of the tensile strength, se Figure 13 (Engström, 2014, ss. 101-102).

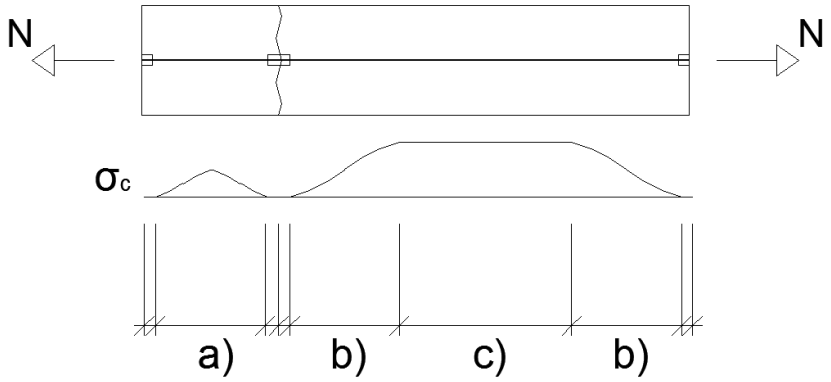

Figure 13 – Cracking process for a reinforced concrete element
a) No risk for another crack to appear, b) the transfer length l_t, c) here there is risk for another crack to appear (Engström, 2014, s. 102).

2.7.4. Thick reinforced bar

For a thin reinforced element, the concrete stress can be assumed to be uniform across the cross section, as the transformation length l_t is longer than the height of the element. This is however not true for a thicker element, which causes a discontinuity region beside the through cracks where the stress is distributed across the cross section This means that further away from the crack in the longitudinal direction, the larger the stress is due to the bonding between reinforcement and concrete. However the amount of concrete where the stress is distributed is increased as well. Therefore the section with maximum tensile stress is somewhere in between, se Figure 14 (Engström, 2014, s. 104).

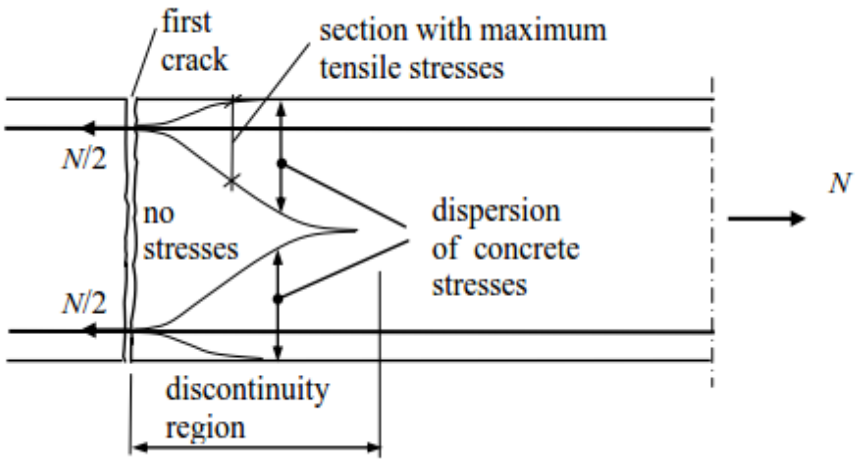

Figure 14 – Stress variation for a thick reinforced concrete element (Engström, 2014, s. 104).

The cracking process will then, after a first through crack has appeared, only consist of small cracks in the highly stressed discontinuity region with the result of Figure 15. It is this cracked region that is described as the effective concrete area $A_{c,eff}$ (Engström, 2014, s. 105).

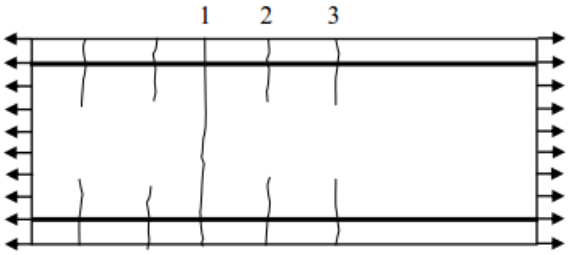

Figure 15 – Cracking for thick reinforced concrete element (Engström, 2014, s. 105).

2.7.5. Type of loading condition

The cracking procedure is highly dependent on the type of loading condition. The two different loading conditions are displacement controlled loading and force controlled loading, and are used for testing the response of a loaded element. A thin reinforced concrete bar is exposed to axial loading with both displacement and force controlled loading as shown in Figure 16.

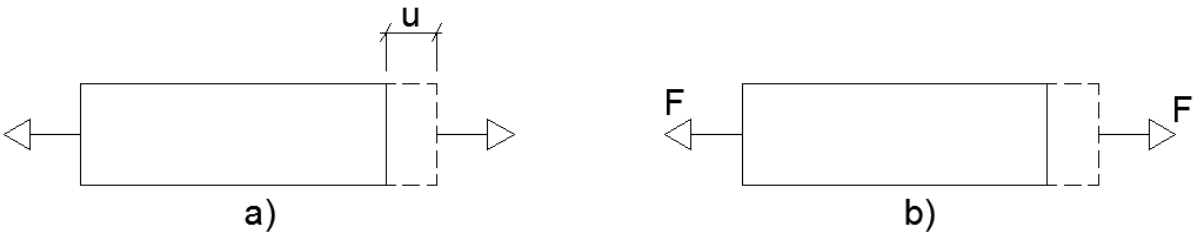

Figure 16 - Thin reinforced concrete bar axially loaded
a) displacement controlled loading, b) force controlled loading

For displacement controlled loading the bar is exposed to small prescribed displacement which is increased with every load step. When the element cracks the stiffness decreases which leads to a drop in internal force. Then the bar must be strained again to achieve the previous internal force. For force

controlled loading the force straining the element is increased by small increments until the element cracks. Then the element will elongate instantaneously, whereas the reinforcement acts as springs, to the current force. This leads to two different behaviours which are shown in Figure 17 (Ghali & Favre, 1994, ss. 326-328) and (Engström, 2014, ss. 106-107).

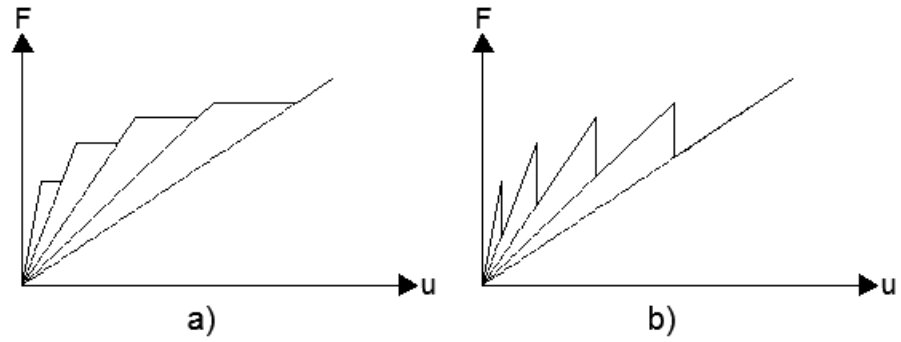

Figure 17 – a) is force controlled loading and b) displacement controlled loading. F is internal force and u is displacement.

2.8. Crack control calculation

To control for cracking in serviceability limit state, FE-calculations are carried out by first assuming a reinforcement area and then calculating the following crack width from the applied forces. If the crack width exceeds the maximum allowable crack width (which is an input parameter) the reinforcement is increased and a new crack width is calculated in an iterative process.

2.8.1. Eurocode 2-1 and 2-2

Maximum allowable crack width w_{max} is decided depending on exposure class, water-cement ratio and the life-span as shown in Table 2.

Table 2 – Lowest allowed concrete cover and max crack width for different exposure classes, max water-cement ration (wcr) and life-span classes (L) (SS 13 70 10, 2002, ss. 4-5).

Exposure class	Max wcr	Lowest allowed concrete cover L100	Lowest allowed concrete cover L50	Lowest allowed cover layer L20	Max crack width L100	Max crack width L50	Max crack width L20
XC0	-	-	-	-	-	-	-
XC1	0.90	15	10	10	0.45	-	-
	0.60	10	10	10			
XC2	0.60	25	20	15	0.40	0.45	-
	0.55	20	15	10			
	0.50	15	10	10			
XC3	0.55	25	20	15	0.30	0.40	-
	0.50	20	15	10			
XC4	0.55	25	20	15	0.30	0.40	-
	0.50	20	15	10			
XS1	0.45	30	25	15	0.20	0.30	0.40
	0.40	25	20	15			
XS2	0.45	50	40	30	0.20	0.30	0.40
	0.40	45	35	25			
	0.35	40	30	25			
XS3	0.40	45	35	25	0.15	0.20	0.30
	0.35	40	30	25			
XD1	0.45	30	25	15	0.20	0.30	0.40
	0.40	25	20	15			
XD2	0.45	40	30	25	0.20	0.30	0.40
	0.40	35	30	20			
	0.35	30	25	20			
XD3	0.40	45	35	25	0.15	0.20	0.30
	0.35	40	30	25			

After that the minimum reinforcement required $A_{s,min}$ can be decided by Equation (2.3) (SS-EN 1992-2, 2005, ss. 34-35).

$$A_{s,min} \cdot \sigma_s = k \cdot k_c \cdot f_{ct,eff} \cdot A_{ct} \tag{2.3}$$

Where:

σ_s Is the stress in the reinforcement
k Is a coefficient which regards the non-uniform self-equilibrating stress
k_c Is a coefficient which regards the stress distribution prior to cracking
$f_{ct,eff}$ Is the mean concrete tensile strength at the time of cracking
A_{ct} Is the concrete area in the tensile zone prior to cracking

Since shrinkage is taken into account $f_{ct,eff}$ should not be lower than 2.9 MPa (SS-EN 1992-2, 2005, s. 36).

Crack calculation is then carried out by calculating the characteristic crack width w_k through Equation (2.4) (SS-EN 1992-1-1, 2005, ss. 122-123).

$$w_k = s_{r,max} \cdot (\varepsilon_{sm} - \varepsilon_{cm}) \tag{2.4}$$

Where:

$s_{r,max}$ Is the maximum crack spacing

$\varepsilon_{sm} - \varepsilon_{cm}$ Is the differential strain between concrete and reinforcement

Where the maximum crack spacing $s_{r,max}$ and the differential strain $\varepsilon_{sm} - \varepsilon_{cm}$ are calculated according by Equations (2.5) and (2.6).

$$s_{r,max} = k_3 \cdot c + \frac{k_1 \cdot k_2 \cdot k_4 \cdot \phi}{\rho_{eff}} \tag{2.5}$$

$$\varepsilon_{sm} - \varepsilon_{cm} = \frac{\sigma_s - k_t \cdot \frac{f_{ct,eff}}{\rho_{eff}} \cdot \left(1 + \alpha_e \cdot \rho_{eff}\right)}{E_s} \geq 0.6 \cdot \frac{\sigma_s}{E_s} \tag{2.6}$$

Where:

k_3 Is a constant given in the Swedish NA
c Is the concrete cover
k_1 Is a coefficient which regards the bond properties of the reinforcement
k_2 Is a coefficient which regards the strain distribution
k_4 Is a constant given in the Swedish NA
ϕ Is the diameter of the reinforcement
ρ_{eff} Is the ratio of $A_s/A_{c,eff}$ due to no pre-stressed reinforcement
A_s Is the area of the reinforcement
$A_{c,eff}$ Is the effective concrete area
k_t Is a coefficient which regards the duration of the load
α_e Is the ratio of E_s/E_c
E_s Is the modulus of elasticity for the reinforcement
E_c Is the modulus of elasticity for the concrete

2.8.2. Andersson & Andersson

Another way to solve this has been developed by Andersson & Andersson (2010). A short 5 step summary is given for restraint loading caused by thermal difference.

1. First the normal force in an element is calculated with regards to both external loads and restraint forces. This is done by first calculating the total deformation δ_{tot} with regards to both external and restraint forces as shown in Equation (2.7).

$$\delta_{tot} = \frac{F + E_c \cdot A \cdot \alpha_{cT} \cdot \Delta T}{\frac{E_c \cdot A}{L} + k} \tag{2.7}$$

Where:

F Is the external force
A Is the cross section area
k Is the spring constant which corresponds the front walls impact on the valve

After that the stress-dependent deformation δ_σ can be calculated as the differential of the total deformation and the stress-independent δ_T as shown in Equation (2.8) where the derivate of the strain-independent deformation is shown in Equation (2.9).

$$\delta_\sigma = \delta_{tot} - \delta_T \tag{2.8}$$

$$\delta_T = \alpha_{cT} \cdot \Delta T \cdot L \tag{2.9}$$

The normal force N can then be calculated according to Equation (2.10)

$$N = \frac{E_c \cdot A}{L} \delta_\sigma \tag{2.10}$$

2. The second part consists of checking if the normal force in the concrete, calculated above, supersedes the tensile strength of the concrete. If it doesn't then the concrete doesn't crack and linear analysis can be made, otherwise the analysis continue below.

3. The restraint force is now separated from the external loads and a fictive stress-dependent strain $\varepsilon_{\sigma,rest}$ can be calculated from the restraint force as shown in Equation 2.11.

$$\varepsilon_{\sigma,rest} = \frac{N_{c,rest}}{E_c \cdot A} \tag{2.11}$$

Where:

$N_{c,rest}$ Is the normal force in the concrete due to restraint forces.

Then it is assumed that the strain in the reinforcement is the same in the concrete due to perfect bonding between concrete and reinforcement which is shown in Equation (2.12).

$$\varepsilon_s = \varepsilon_{\sigma,rest} \tag{2.12}$$

4. From the reinforcement strain and additional stress $\sigma_{s,add}$ is calculated from Equation (2.13)

$$\sigma_{s,add} = \varepsilon_s \cdot E_s \tag{2.13}$$

5. The additional stress is then added to the stress from external loading. Subsequent design is then carried out according to EC 2-1 and EC2-2.

For a more detailed description, see Andersson & Andersson (2010).

3. Method

3.1. General

The investigation process was carried out in three steps. First technical drawings of concrete slab frame bridges were collected from BaTMan. These bridges were then modelled with the FE-program SOFiSTiK. The reinforcement need was calculated in the serviceability limit state with only permanent loads and restraint forces for the different reinforcement models. Finally the bridges were also investigated in the field in according to bridge inspection practice for ocular examination.

3.2. BaTMan

The bridges that were collected from BaTMan were chosen from the following criteria.

- Accessibility
  Only bridges that were not crossing water or train tracks were chosen due to accessibility consideration.

- Proximity
  Only bridges in the vicinity of Lund Municipality and the City of Malmö were chosen.

- Construction type
  Only single span concrete slab frame bridges were chosen. Furthermore only road bridges were chosen.

The following bridges which were collected from BaTMan are shown in Table 4.

Table 3 – Investigated bridges in Lund Municipality and the city of Malmö.

Municipality	ID Nr.	Swedish name	Const. year
Malmö	12-404-1	Bro över enskild väg vid Kronetorp	1953
Malmö	12-438-1	Bro över allmän väg vid Tygelsjö	1972
Malmö	12-598-1	Bro över allmän väg vid Petersborg i Malmö, broläge 16	1972
Lund	12-604-1	Bro över gång- och cykelväg, 2.0 km nv Lunds domkyrka	1972
Lund	12-605-1	Bro över gång- och cykelväg, 1.9 km n Lunds domkyrka	1970
Lund	12-606-1	Bro över gång- och cykelväg, 1.9 km no Lunds domkyrka	1970
Lund	12-650-1	Bro över gc-väg vid Boställsvägen, N Ringen i Lund	1972
Lund	12-921-1	Bro över Sölvegatan s tpl Lund n	1982
Lund	12-926-1	Bro över enskild väg vid Ladugårdsmarken i Lund	1982
Lund	12-927-1	Bro över enskild väg 1.1 km s Odarslövs k:a (gamla)	1993
Lund	12-1374-1	Bro över GC-väg N tpl Råby	2009

The bridges were then grouped into different groups depending on which type of bottom plate used, whether the valve was angled or not and what type of road the bridge crosses. An open bottom plate will be exposed to support settlement unlike the closed bottom plate. A skewed angled valve will have larger transversal reinforcement as the reinforcement isn't placed in the same direction as the principal moment. Bridges that crosses a pedestrian/bicycle path will have a larger crack width allowance for the sides of the front walls and valve that borders the road then a bridge that crosses a car road. This is due to the different exposure classes of the road types. The grouping is shown in Table 5.

Table 4 – Bridge groups.

ID Nr.	Bottom plate	Skewed angled valve	Crossing road type
12-404-1	Open	Yes	Car road
12-438-1	Open	No	Car road
12-598-1	Open	Yes	Car road
12-604-1	Open	Yes	Pedestrian/cycle path
12-605-1	Closed	Yes	Pedestrian/cycle path
12-606-1	Open	Yes	Pedestrian/cycle path
12-650-1	Open	No	Pedestrian/cycle path
12-921-1	Open	Yes	Car road
12-926-1	Open	No	Car road
12-927-1	Open	Yes	Car road
12-1374-1	Closed	Yes	Pedestrian/cycle path

3.3. FE-Analysis

The design approach for the FE-Analysis is described below through two examples, bridge 12-1374-1 and 12-604-1. The technical drawings for the two bridges are available in Appendix 3.

Bridge 12-1374-1 is located where the E22 crosses a pedestrian and bicycle path just north of interchange Råby in Lund. Some general data for the bridge is summarised below in Table 6.

Table 5 - General information for bridge 12-1374-1.

General Information	
Road nr:	E22
Municipality / City:	Lund
Constructions year:	2009
Span:	7.4 m
Width:	35.9 m
Design firm:	Centerlöf & Holmberg

Bridge 12-604-1 is located where the E6.02, in popular speech called Norra Ringen, crosses a pedestrian and bicycle path just south west of the Oskarshem park in Lund. Some general data for the bridge are summarised below in Table 7.

Table 6 – General information for bridge 12-604-1.

General Information	
Road nr:	E6.2
Municipality / City:	Lund
Constructions year:	1972
Span:	6.3 m
Width:	27 m
Design firm:	Statens Vägverk

3.3.1. Geometry

First the geometry for the bridges in according was created according to the dimensions found in the technical drawings, see Figures 18 & 19. One simplification was made namely that the edge beam was not modelled due to their impacts on restraint forces is negligible.

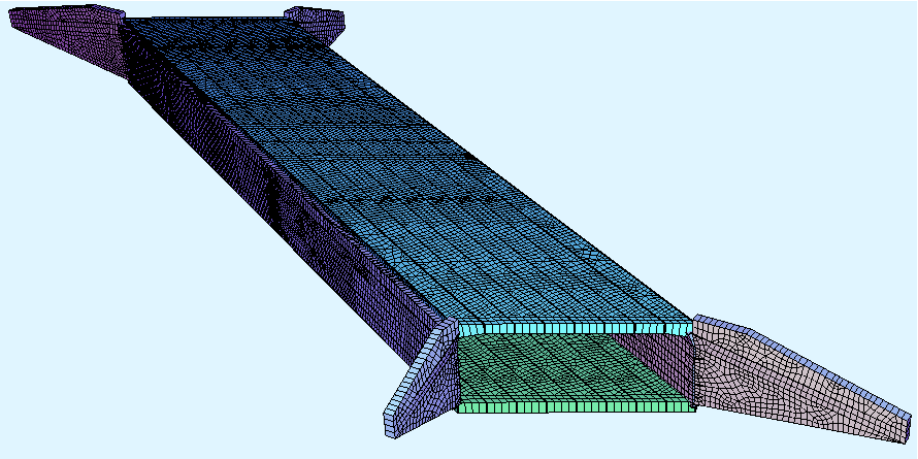

Figure 18 – Meshed figure of 12-1374-1.

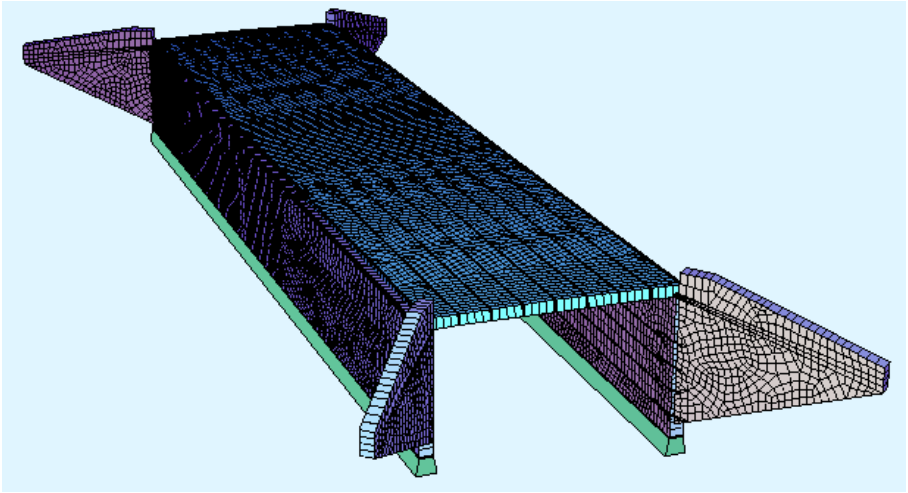

Figure 19 – Meshed figures of 12-604-1.

The supports were modelled differently depending on which type of bottom plate was used. For a closed bottom plate a bedding modulus of 16 MN/m^3 was applied to the plate according to praxis. For the closed bottom plate the plates was modelled as beams connected to a single support with a rotation stiffness corresponding the bedding modulus.

After the geometry was created, loads acting on the structure were added. The added loads were permanent loads, support settlement for bridge with an open bottom plate and temperature.

3.3.2. Permanent loads – self-weights

The concrete self-weight was accounted for by applying a volume load of 25 kN/m^3 (the weight of reinforced concrete) to the entire superstructure. Furthermore the elasticity of the concrete was reduced by 40 % according to praxis to take account for the expected cracking. The self-weight load of the pavement was calculated by applying an area load on the valve which equals the weight of the pavement multiplied with the height of the pavement. The height of the pavement was taken from the technical drawings and the heaviness of the pavement was set to 23.5 kN/m^3 as this is the mean value of the most common pavement weight namely asphalt concrete and mastic asphalt (TRVK Bro 11, 2011, s. 43). The self-weight of the pavement was calculated for two load cases, one where the load was increased by 10 % and one where the load was decreased by 10 % (TRVFS 2011:12, 2011, s. 9).

3.3.3. Permanent loads – earth pressure

The lateral earth pressure load g_{ep} is calculated as an area load according to Equation 3.1 (Sällfors, 2009, s. 9.4).

$$g_{ep} = K_0 \cdot \sigma_{ep} \tag{3.1}$$

Where:

K_0	Is the lateral earth pressure coefficient at rest
σ_{ep}	Is the vertical earth pressure

To determine the earth pressure, the type of backfill used was taken from the technical drawings. For both example bridges gravel material was used as backfill. The characteristic friction angle for gravel material was taken from table 5.2-3 in TK Geo 2013 and was found to be 45°, and the weight was taken from table 5.2-1 in TK Geo 2013 and was found to be 22 kN/m^3. The design value for the friction angle equals the characteristic value in the serviceability limit state (TRVFS 2011:12, 2011, s. 56). With the design friction angle known the coefficient of lateral earth pressure at rest K_0 was calculated according to Equation 3.2 (TK Geo 11, 2011, s. 36):

$$K_0 = 1 - \sin(\phi_d) \tag{3.2}$$

For the wing walls the coefficient of lateral earth pressure at rest K_0 must be modified as the soil level behind the wing wall is inclined upwards. This was done according to practice by replacing $K_0$with K_0^* calculated according to Equation 3.3 (Kamrad, 2016).

$$K_0^* = K_0 \cdot (1 + \sin(\beta)) \tag{3.3}$$

Where β is the angle of the slope behind the wing wall. A schematic picture of the lateral earth pressure at rest is shown in Figure 20 where a) is showing a 2D picture and b) is showing a 3D picture.

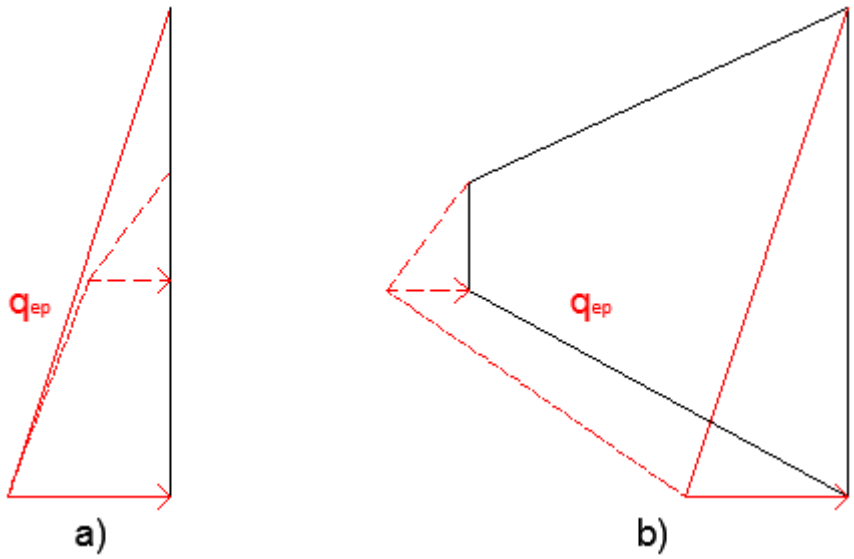

Figure 20 - Lateral earth pressure at rest (red lines) on wing walls (black lines). Observe that the earth pressure on the end of the wing walls, the dashed lines, has a greater slope due to the inclination of the earth slope behind it.

3.3.4. Permanent loads – shrinkage & creep

For closed bottom plate bridges the bottom plate is assumed to be able to able to shrink unhindered. As the front walls and valve is cast later the bottom plate will restrain the front walls from shrinking fully. The shrinkage load is thus calculated through practice by applying a $10°C$ load on the front walls, wings and the valve (Bro 2004, 2004, s. 8). For the open bottom plate bridges the entire structure is assumed to be fixed. Thus the full shrinkage load, which through practice is set to $25°C$, is applied on the entire structure (Kamrad, 2016).

The effect of creep is taken into account by applying a reduction factor on the shrinkage and temperature load which give rise to normal forces. The effect of creep is calculated from the creep constant φ, which through practice is set to 2 for shrinkage and 0.3 for temperature loads (Kamrad, 2016).

3.3.5. Support settlement

For bridges with multiple supports, settlement must be taken into account. For horizontal support settlement the design value is allowed to be assumed to 10 mm. For vertical support settlements the design support settlement shall be calculated as the difference between the design settlements for support one minus the characteristic settlement for support two (TRVR Bro 11, 2011, s. 26). A differential settlement of 20 mm gives a good approximation for most bridges (Kamrad, 2016) and is used in this thesis. The displacements are applied on the supports as shown in Figure 21. All the support settlements are calculated separately but only the worst one of them is used in the load combination.

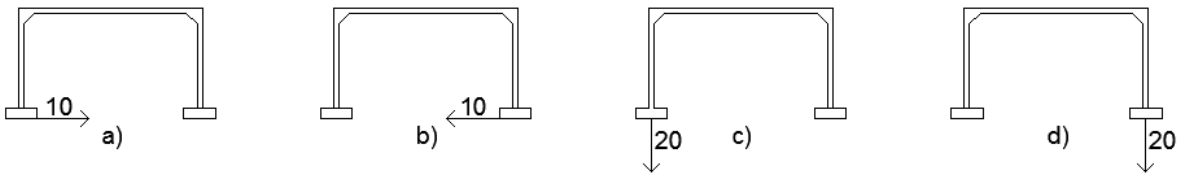

Figure 21 – Support settlements. a) and b) are showing the horizontal settlement and c) and d) are showing the vertical settlement.

3.3.6. Thermal loads

The thermal loads are calculated by both applying an evenly distributed thermal component T_N as well as a vertical linear temperature difference T_M (SS-EN 1991-1-5, 2003, s. 17).

The evenly distributed thermal component is calculated from the maximum/minimum air temperature found in appendix 2 of the NA (TRVFS 2011:12, 2011, s. 77). As both bridges are in the vicinity of Lund, the max/min air temperatures was read to $34/-23\ °C$. The evenly distributed thermal component was then read from Figure 6.1 in SS-EN 1991-1-5, which gave the maximal/minimal evenly distributed thermal component as $35/-15\ °C$. Finally the characteristic evenly distributed thermal component which causes contraction $\Delta T_{N,con}$ and the characteristic even distributed thermal component which causes expansion $\Delta T_{N,exp}$ was calculated depending on the bridge temperature at casting T_0 (SS-EN 1991-1-5, 2003, s. 19). As the initial temperature of the bridges was unknown, it's practice to set T_0 to $10\ °C$ (SS-EN 1991-1-5, 2003, s. 30). This gives the characteristic even distributed thermal components to $25/-25\ °C$ for both bridges. Furthermore an additional $15°C$ difference between the valve and the front walls was applied (SS-EN 1991-1-5, 2003, s. 25).

The linear temperature differences $\Delta T_{M,heat}$ and $\Delta T_{M,cool}$ are set for concrete slab bridges to $15°\ C$ if it's warmer above the valve surface ($\Delta T_{M,heat}$) and $-8°\ C$ if it's warmer under the valve surface

($\Delta T_{M,cool}$) (SS-EN 1991-1-5, 2003, s. 20). These values are then modified depending on the thickness of the pavement in according to Table 6.1 in SS-EN 1991-1-5. For bridge 12-1374-1 the temperature difference is set to 10.5 if it's warmer above the surface and 8 if it's warmer under the surface and for bridge 12-604-1 the temperature difference is to 10.5 if it's warmer above the surface and to 8 if it's warmer under the surface.

To take account into simultaneous effects, the temperature load should be combined into the following eight load cases (SS-EN 1991-1-5, 2003, s. 25).

Load case 1: $\Delta T_{M,heat} + 0.35 \cdot \Delta T_{N,exp}$

Load case 2: $\Delta T_{M,heat} + 0.35 \cdot \Delta T_{N,con}$

Load case 3: $\Delta T_{M,cool} + 0.35 \cdot \Delta T_{N,exp}$

Load case 4: $\Delta T_{M,cool} + 0.35 \cdot \Delta T_{N,con}$

Load case 5: $0.75 \cdot \Delta T_{M,heat} + \Delta T_{N,exp}$

Load case 6: $0.75 \cdot \Delta T_{M,heat} + \Delta T_{N,con}$

Load case 7: $0.75 \cdot \Delta T_{M,cool} + \Delta T_{N,exp}$

Load case 8: $0.75 \cdot \Delta T_{M,cool} + \Delta T_{N,con}$

As the front walls press against the backfill due to temperature increase in the valve an increase of lateral earth pressure must be taken into account (TRVK Bro 11, 2011, s. 54). This is done by adding a triangular horizontal load with the value Δp, calculated by Equation 3.4, as the maximum value in the centre of the front wall. (TRVR Bro 11, 2011, s. 28).

$$\Delta p = c \cdot \gamma \cdot z \cdot \beta \tag{3.4}$$

Where:

- c Is the cohesion constant which equals to 600 for unfavourable load
- γ Is the weight of the earth
- z Is the depth from the top of the front wall
- β Is the ratio of the displacement, due to the temperature, divided with the height of the front wall

Equation 3.4 can then be rewritten to Equation 3.5:

$$\Delta p = c \cdot \gamma \cdot \frac{1}{2} \cdot (T_{max} - T_{min}) \cdot \alpha_{cT} \cdot \frac{L}{2} \tag{3.5}$$

Where:

- L Is the span length

A schematic 3D-picture of the additional earth pressure is shown in Figure 22.

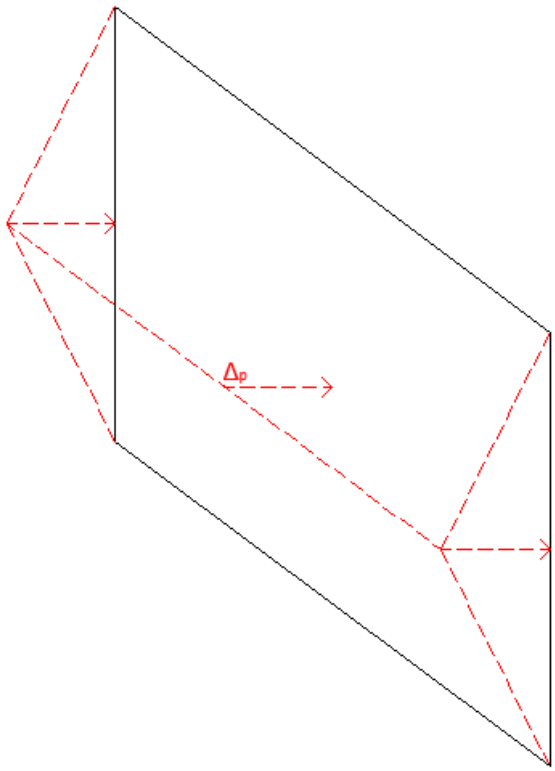

Figure 22 – Additional earth pressure (red lines) on a front wall (black lines).

3.3.7. Concrete cover and crack width

The different parts of the bridge structure must be designed with a prescribed maximum crack allowance as well as a lowest allowed concrete cover. These parameters are dependent on the life span of the structure, the water-cement ratio and the exposure class of the area.

For bridge 12-1374-1 the lowest allowed concrete cover was set to 40 mm for the entire structure except at the bottom of the bottom plate and the edge beams where a layer of 50 mm was prescribed. The service life was set to 80 years and the water-cement ratio was set to ≤40. As the crossed road was a pedestrian/bike path the exposure class was set to XD1. This gave an allowable crack width of 0.3 mm for the bottom of the valve and the inner side of the front wall.

For 12-604-1 the lowest allowed concrete layer was prescribed to 30 mm except at the bottom of the bottom plate where 100 mm was prescribed. Neither the service life nor the water-cement ratio was set in the technical drawin, so a maximum allowable crack width of 0.3 was assumed as the bridge crossed over a pedestrian/bike path.

3.3.8. Skewed bridges

For some skew angled bridges the longitudinal reinforcement in the valve is placed in a fan geometry as shown in Figure 23.

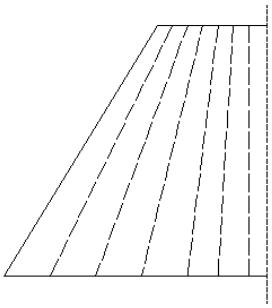

Figure 23 - Fan placement of reinforcement (dashed lines) in a skew area of the valve as seen from above.

For these areas with skew reinforcement the maximum moment for the reinforcement need to be recalculated according to Equations (3.6) and (3.7) (TRVR Bro 11, 2011, s. 51). This must be done as a skewed longitudinal reinforcement will give rise to an increased need of transversal reinforcement.

$$M_x = \frac{1}{\sin^2\psi}[M_1 \sin^2(\psi-\delta) + M_2 \cos^2(\psi-\delta) \pm |M_1 \sin\delta \sin(\psi-\delta) - M_1 \sin\delta \sin(\psi-\delta)|] \quad (3.6)$$

$$M_y = \frac{1}{\sin^2\psi}[M_1 \sin^2\psi + M_2 \cos^2\delta \pm |M_1 \sin\delta \sin(\psi-\delta) - M_1 \sin\delta \sin(\psi-\delta)|] \quad (3.7)$$

Where:

M_x & M_y	Are the design moments for the reinforcement.
M_1 & M_2	Are the principal moments.
δ & ψ	Are angles between the principal moments and the reinforcement.

A descriptive picture of the skewed reinforcement against the principal moment is shown in Figure 24.

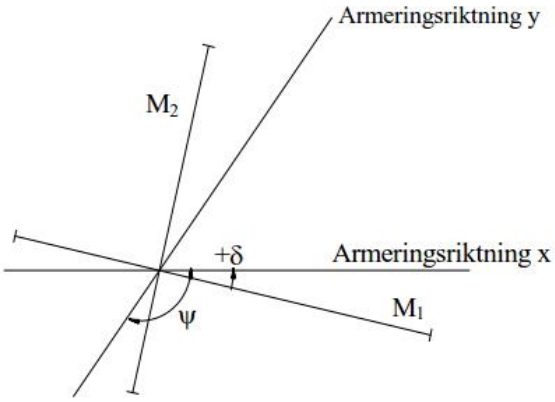

Figure 24 - Skewed reinforcement direction (sv: Armeringsriktning) and principal moments (TRVR Bro 11, 2011, s. 51).

It is “impossible” to account for a continuous increase of skewing of the reinforcement in the computer calculations. Therefore the transversal reinforcement need is calculated twice for bridges that are skewed. Once where longitudinal reinforcement is placed perpendicular to the transversal and once where the longitudinal reinforcement is placed with the maximum skew angle.

3.4. Field investigation

The field investigation was carried out according to the rules of ocular examination from the Swedish Swedish Road Administrations handbook for bridge inspection (Vägverket, 1993). This meant that the bridges were inspected with a ruler and all visible cracks had their width measured and place documented.

4. Results

4.1. General

Only the results for bridge 12-1374-1 and 12-604-1 are presented in this chapter, the rest can be found in Appendix 1 with photos of the cracks in Appendix 2. Furthermore, the results for the bridges here are presented thoroughly whereas only the FEA and ocular examination are presented for the bridges in the appendix. At the end of the chapter a table with all the summarised results is shown.

First the FE-design results for one of the front walls and the valve are shown and after that the results from the ocular examinations are shown.

4.2. Results for 12-604-1

First a schematic picture is presented which explains the amount of transversal reinforcement needed as prescribed by the technical drawings. The picture is divided in different zones where the amount of reinforcement differs, see Figure 25 and 26.

Furthermore only the side that is visible from the tunnel is presented, meaning the inner side of the front walls and the bottom of the valve. This is due to these being the only sides which can be inspected.

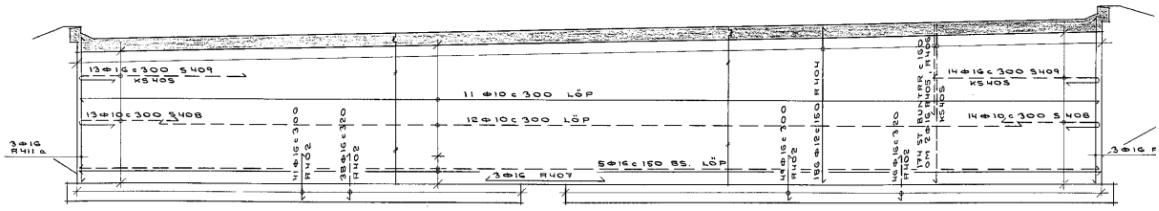

Figure 25 - Reinforcement drawing for the front wall of bridge 12-604-1.

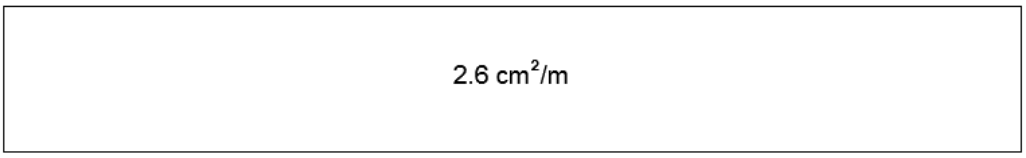

Figure 26 - Schematic drawing of the transversal reinforcement from Figure 25. Only the reinforcement need for the side towards the tunnel (the dashed reinforcement lines in figure 25) is shown.

Following that the theoretically needed reinforcement is presented. To make the comparison between the schematic picture and calculated reinforcement easier, only the values exceeding the present reinforcement are shown. Furthermore the results from the Andersson & Andersson method are placed to the right and the results from the Eurocode method are placed to the left, se Figure 27.

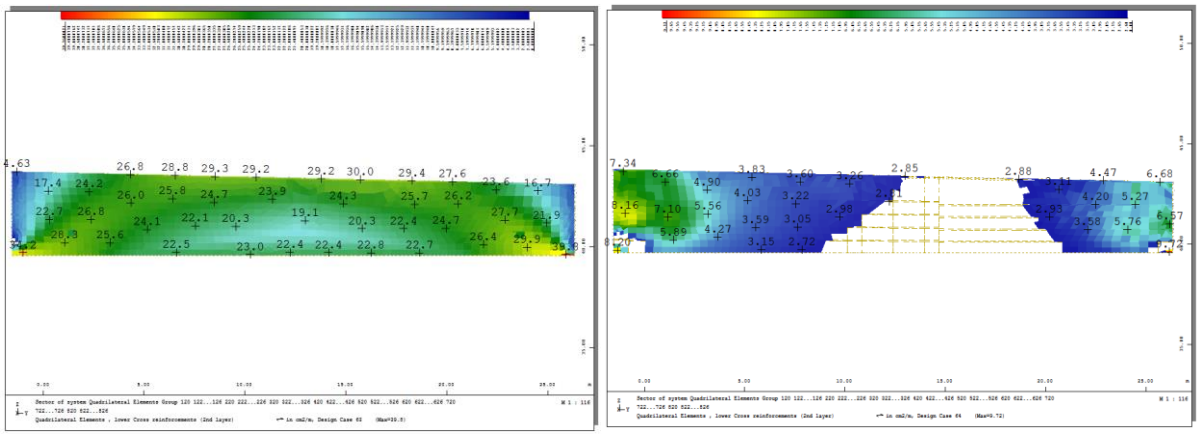

Figure 27 –
Left: Theoretical reinforcement need for the front wall calculated with the Eurocode method with reinforcement that exceeds 2.6 cm^2/m cut out.
Right: Theoretical reinforcement need for the front wall calculated with the Andersson & Andersson method with reinforcement that exceeds 2.6 cm^2/m cut out.

Below the technical drawing and a schematic picture of the valve is presented, see Figures 36 and 37.

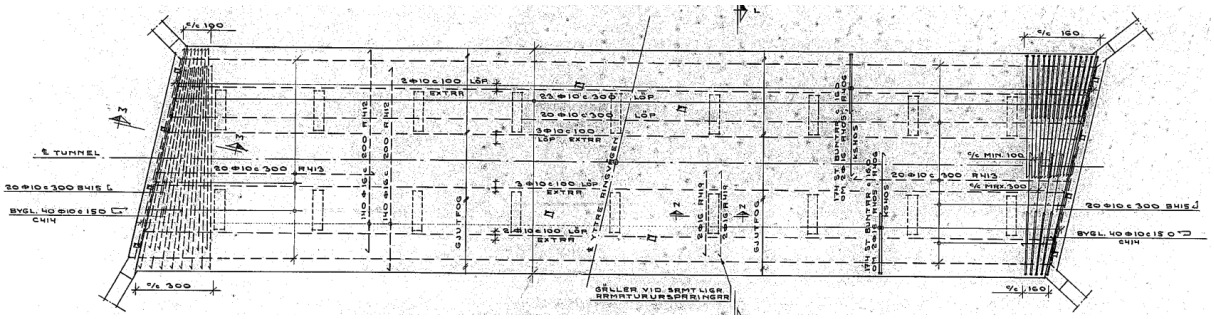

Figure 28 - Reinforcement drawing for the valve of bridge 12-604-1.

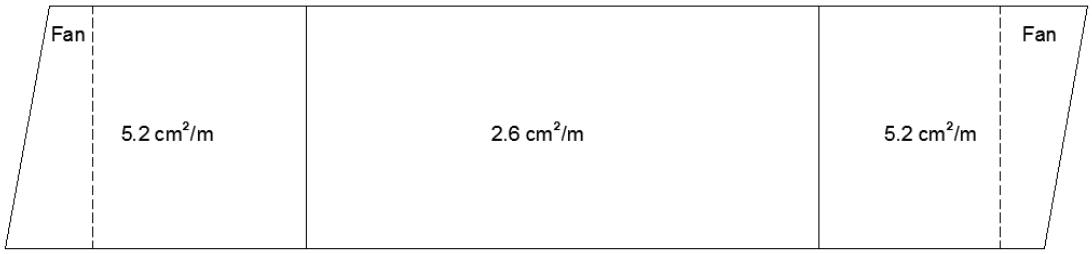

Figure 29 – Schematic drawing of the transversal reinforcement from Figure 28. Only the reinforcement need for the side towards the tunnel (the dashed reinforcement lines in figure 28) is shown. Observe that the zones where the longitudinal reinforcement is placed with a fan geometry is shown.

Here the reinforcement need must be calculated twice. Firstly the longitudinal reinforcement was placed orthogonal to the transversal reinforcement, see Figure 30, and is thus valid for the non-fan zone. Secondly the reinforcement need was calculated with skewed longitudinal reinforcement placement, see Figure 31, and is thus valid for the fan zone.

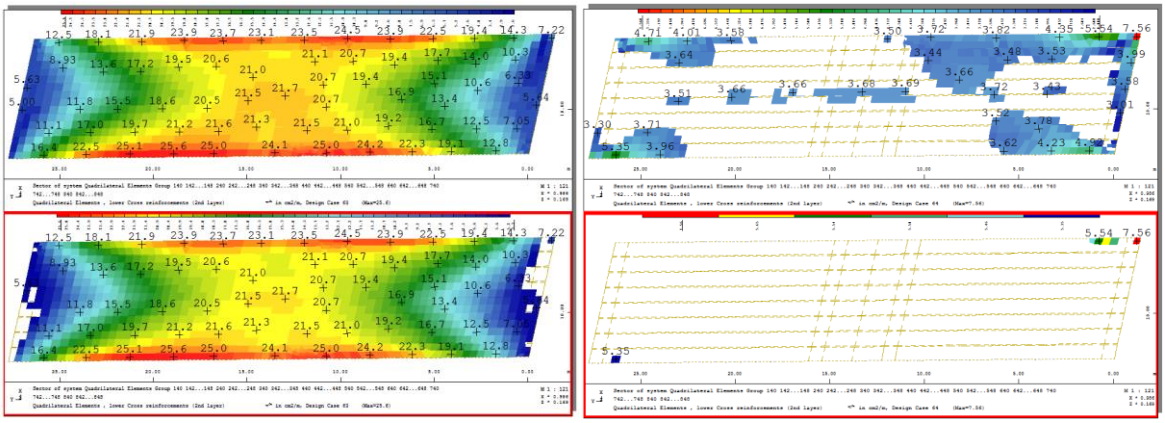

Figure 30 –
Upper left: Theoretical reinforcement need for the valve calculated with the Eurocode method with reinforcement that exceeds 2.6 cm^2/m.
Lower left: Theoretical reinforcement need for the valve calculated with the Eurocode method with reinforcement that exceeds 5.2 cm^2/m.
Upper right: Theoretical reinforcement need for the valve calculated with the Andersson & Andersson method with reinforcement that exceeds 2.6 cm^2/m.
Lower right: Theoretical reinforcement need for the valve calculated with the Andersson & Andersson method with reinforcement that exceeds 5.2 cm^2/m.

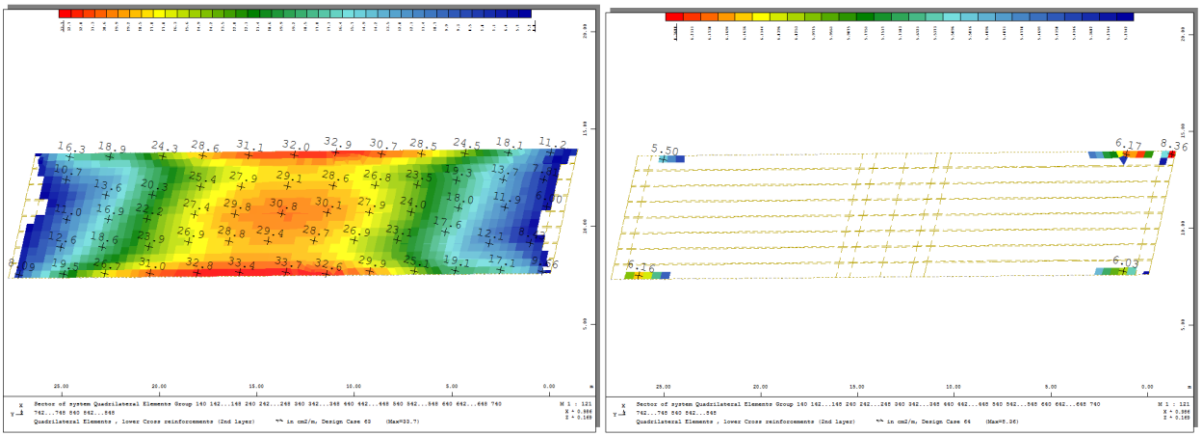

Figure 31 –
Left: Theoretical reinforcement need for the valve calculated with the Eurocode method with reinforcement that exceeds 5.2 cm^2/m cut out.
Right: Theoretical reinforcement need for the valve calculated with the Andersson & Andersson method with reinforcement that exceeds 5.2 cm^2/m cut out.
Observe that the text in the figure is angled. This is an error in SOFiSTiK where the text for the transversal reinforcement is always placed orthogonally to the longitudinal reinforcement direction and not in the direction of transversal reinforcement.

After the FEA results the result of the ocular inspection is presented in a Figure showing a schematic picture of the cracking of the front wall, se Figure 32, and the valve, se Figure 33. Cracks that were measured will have their width written and cracks exceeding the allowable crack width will be bolded.

Observations in the field yielded the following results:

- The interior of the tunnel was heavily painted so it was hard to both detect cracks as well as to decide the crack width. Observation also showed that both the front wall and the valve were cast in three phases, with two construction joints.
- Minor cracks were observed in the outer cast stages and a clear continuous larger crack was observed in the middle of the centre cast phase, see Figure 32.
- Only hints of longitudinal cracks going between the light installation and the front walls, see Figure 33.

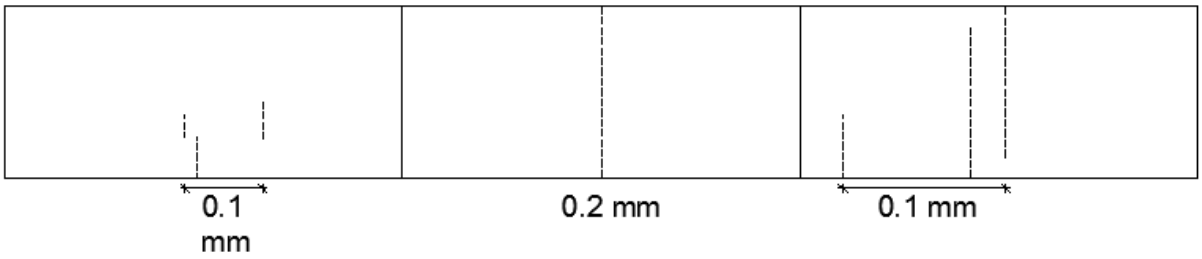

Figure 32 – Observed cracks in the front wall.

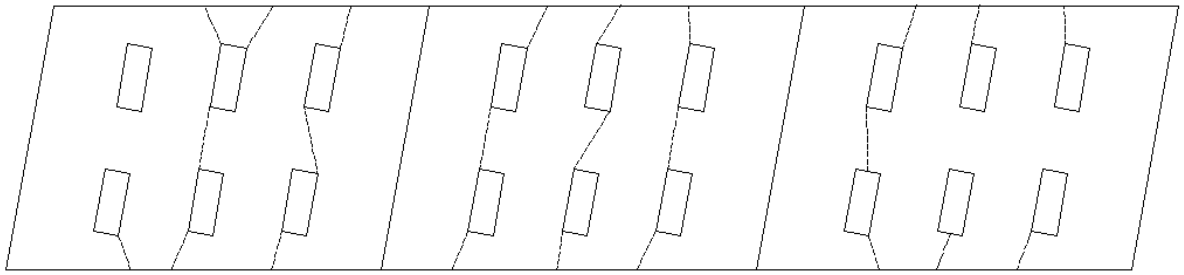

Figure 33 - Observed cracks in the valve.

4.3. Results for 12-1374-1

The present reinforcement amount in the front wall is presented in Figure 34. Observer that the reinforcement need is higher in the left side of the front wall.

Figure 34 – Present reinforcement for the front wall according to technical drawing.

The calculated reinforcement need for the front wall is presented in Figure 35.

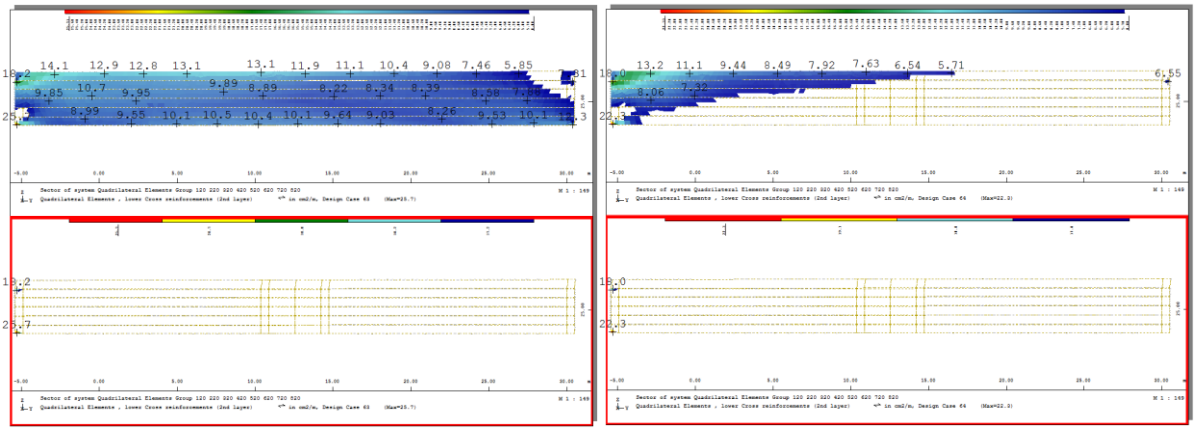

Figure 35 –
Upper left: Theoretical reinforcement need for the front wall calculated with the Eurocode method with reinforcement that exceeds 5.7 cm²/m.
Lower left: Theoretical reinforcement need for the front wall calculated with the Eurocode method with reinforcement that exceeds 15.7 cm²/m.
Upper right: Theoretical reinforcement need for the front wall calculated with the Andersson & Andersson method with reinforcement that exceeds 5.7 cm²/m.
Lower right: Theoretical reinforcement need for the front wall calculated with the Andersson & Andersson method with reinforcement that exceeds 15.7 cm²/m.

The present reinforcement amount in the valve is presented in Figure 37 for the non-fan zone and 38 for the fan zone. Observe that the fan zone is covering a bit of the 5.7 cm²/m zone.

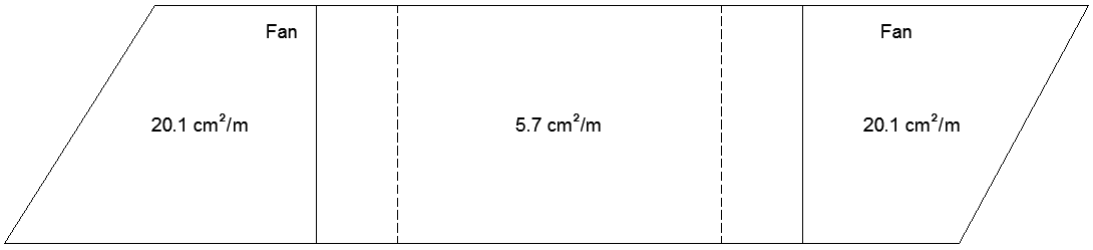

Figure 36 – Present reinforcement for the valve according to technical drawing.

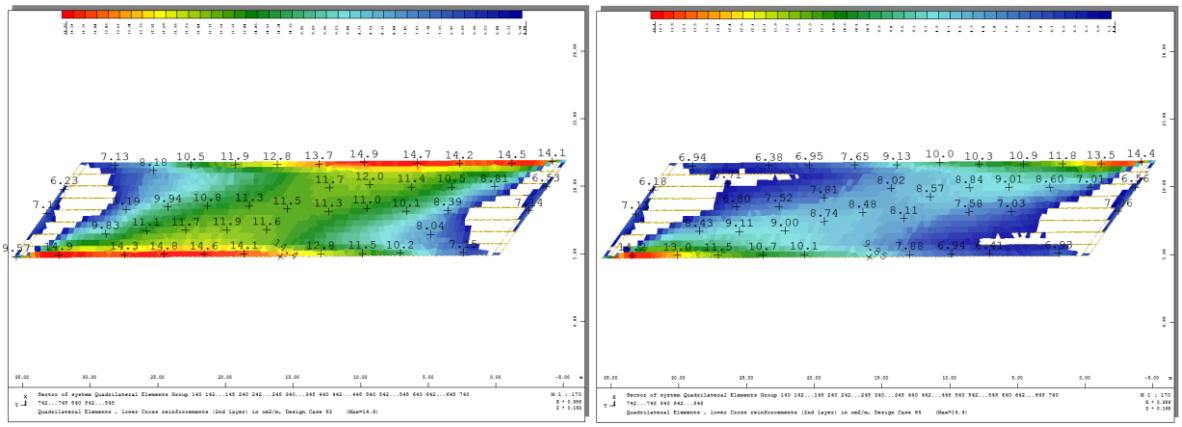

Figure 37 – Orthogonal reinforcement need for the valve. Results below 5.7 cm^2/m are cut out.

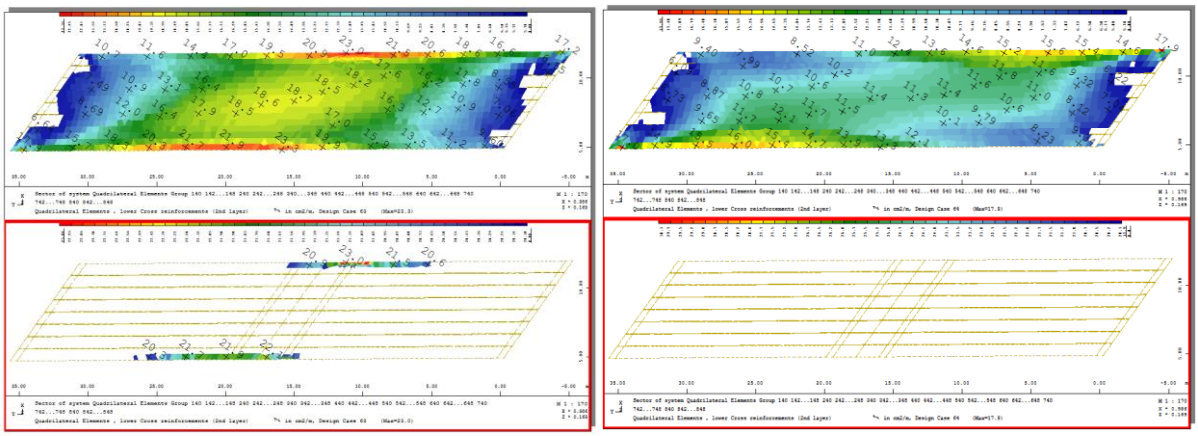

Figure 38 – Skewed reinforcement need for the valve. Results below 5.7 and 20.1 cm^2/m are cut out.

Observations in the field yielded the following results:

- No cracks found in the front wall.
- No cracks found in the valve.

4.4. Summarized results

To make comparison between the bridges easier, data for the centre of the front wall and valve are presented in Table 8 & 9. The data shown is present reinforcement, calculated maximum reinforcement need, max allowable crack width and observed crack width.

Table 7 - Results for centre of front walls

Bridge Nr.	Present reinforcement (cm^2/m)	Eurocode method (cm^2/m)*	A&A method (cm^2/m)*	Allowable crack width (mm)	Field observations (mm)
12-404-1	2.6	54.0	4.46	0.2	0.1
12-438-1	2.6	31.5	3.96	0.2	0.1
12-598-1	8.9	39.3	<8.9	0.2	None observed
12-604-1	2.6	29.2	2.85	0.3	0.2
12-605-1	2.6	9.36	5.65	0.3	**2.0**
12-606-1	2.6	28.6	<2.6	0.3	0.2
12-650-1	2.6	29.1	<2.6	0.3	0.2
12-921-1	5.7	40.6	<5.7	0.2	**0.3**
12-926-1	7.9	42.7	<7.9	0.2	0.2
12-927-1	5.6	49.2	9.22	0.2	Not investigated
12-1374-1	15.7	<15.7	<15.7	0.3	None observed

Table 8 - Results for centre of the valve

Bridge Nr.	Present reinforcement (cm^2/m)	Eurocode method (cm^2/m)	A&A method (cm^2/m)	Allowable crack width (mm)	Field observations (mm)
12-404-1	6.5	55.8	9.28	0.2	None observed
12-438-1	2.6	29.3	5.39	0.2	None observed
12-598-1	11.3	34.8	<11.3	0.2	Crack not measured**
12-604-1	2.6	24.1	3.68	0.3	Crack not measured**
12-605-1	2.6	8.57	7.01	0.3	Crack not measured**
12-606-1	2.6	28.3	4.21	0.3	Crack not measured**
12-650-1	2.6	25.5	3.81	0.3	Crack not measured**
12-921-1	5.7	60.2	7.56	0.2	None observed
12-926-1	3.3	38.9	5.82	0.2	None observed
12-927-1	10.1	23.1	11.7	0.2	Not investigated
12-1374-1	5.7	14.9	10.1	0.3	None observed

*** The values shown here are the peak values found in the centre of the element.**

**** Optical appearances indicated that the all crack widths was <0.3 mm.**

5. Discussion

From the results the following statements can be made regarding the issues asked in the beginning.

1. Only one bridge (12-921-1) had a crack in the front wall that exceeded the crack allowance. All other bridges had cracks within their acceptable crack width. As the crack width of the valve cracks was not measured it's difficult to say anything absolute about if cracking in the valve is a problem or not. However, the cracks observed were believed to vary along 0.1 to 0.3 mm.

2. One might have suspected that the closed bottom plate bridges would need more reinforcement as they have an additional load from the support settlement but this wasn't the case. Bridge 12-605-1 had roughly the same amount of cracks and crack width as the adjacent open bottom plate bridges, disregarding the huge 2.0 mm crack in bridge 12-605-1. The reason that no cracks could be found in bridge 12-1374-1 is probably that it's a new bridge, constructed 2009, where modern safety factors was applied for the reinforcement calculations. Alternatively, restraint forces might not be fully developed yet.

   Two skewed bridges (12-404-1 & 12-598-1) had the same amount of reinforcement through the entire valve but with different crack results. 12-404-1 had two large cracks at the sides as could be expected because of the increased moment in the reinforcement direction. However bridge 12-598-1 only had a crack in the middle where the reinforcement is placed orthogonally.

   Cracking in the valve was more common on the pedestrian/bike path bridges than on the road bridges where there was only one bridge (12-598-1) where cracks where observed. This can however depend on the large amount of light fixtures installed on the pedestrian/bike path bridges. For the front walls the number of cracks was significantly higher for the pedestrian/bike path bridges. There the number of cracks varied between 0-20 while for the car road bridges the number of cracks varied between 4-8. The cracks were also more tightly placed for the pedestrian/bike path bridges where multiple cracks could be found on the same cast phase. Finally only the car road bridges had horizontal cracks in the front walls.

3. For the Eurocode method the calculated theoretical need can be up to 20 times higher than the present adequate reinforcement. The Andersson and Andersson method gives much more reasonable values that in some cases can give an overestimation up to two times higher than the present reinforcement.

5.1. Sources of errors

A number of identifies errors, uncertainties and assumption made in the thesis are presented below.

- It is the outside of the front walls, towards the earth, where cracking is dangerous. This is due to ground water being able to penetrate the cracked concrete cover and transport chemicals, such as chlorine, to the uncovered reinforcement.

- Measuring the crack width with a ruler is very arbitrary. The width measured could easily differ by 0.1 mm. Additionally the crack width also varies along the crack length.

- All through cracks above 0.2 mm shall be repaired by injection (Vägverket, 1993). This means that some bridges may have cracked a lot more due to shrinkage or support settlement but have been repaired before they were inspected.

- There are a lot of assumptions made in the FEA. First in the shrinkage calculations it is assumed that the open bottom plate bridges will shrink to a corresponding $25°C$ change in temperature. Whether the bridges have done this in reality is impossible to verify. Secondly all open bottom plate bridges are assumed to have settled. To verify if they have is also impossible. Finally the elasticity of the concrete was reduced by 40 % to account for the cracking. Even though this is common praxis and assumed reasonable it's difficult to verify that it's true for all the calculated bridges.

- All crack discovered here are assumed to be due to restraint forces, with the exception of the 2.0 crack in 12-605-1. The horizontal cracks in 12-438-1 12-958-1 might be caused by the traffic load.

5.2. Further research

Although this thesis answers the main question asked in the beginning of the thesis it leaves a few questions unanswered. These questions would make good as future research subjects.

- The cracks identified were all assumed to be due to restraint forces. Is this true? It is possible to distinguish between shrinkage and thermal cracks?

- The bridges here were only inspected once. How does the crack width change over time/temperature?

- Due to time restraint only the Andersson and Andersson method was compared to the results from the Eurocode method. The results could have been compared to the results from the method developed by (Kamali, Johansson, & Svedholm, 2013) or a proper non-linear analysis.

6. Conclusion

The conclusions which can be made from the report are.

- Although very common cracking is not a problem for existing Swedish concrete slab frame bridges.

- No correlation can be made regarding the different bottom plates and the concrete cracks. However, due to the low number of investigated closed bottom plate bridges this isn't certain.

- No correlation regarding the impact of the skew can be made.

- There is a correlation between what type of road a bridge crosses and how the cracking is developed in the bridge. Bridges that crossed bike/pedestrian paths had more cracks compared to the bridges that crossed car roads. However, only horizontal cracks could be found on the bridges that crossed car roads.

- For the FEA, the Andersson & Andersson method gives results that are more reasonable than the Eurocode method.

7. References

Alfredsson, H., & Spåls, J. (2008). *Cracking Behaviour of Concrete Subjected to Restraint Forces.* Gothenburg, Sweden: Chalmers University of Technology.

Andersson, J., & Andersson, L. (2010). *Tvångskrafter i betongbroar - Analys och implementering av metod för reducering av tvångskrafter.* Lund, Sweden: Lunds University.

Bro 2004. (2004). *Bro 2004.* Borlänge, Sweden: Swedish Road Administration (now part of Swedish Transport Administration).

Engström, B. (2014). *Restraint cracking of reinforced concrete structures.* Gothenburg, Sweden: Chalmers Univeristy of Technology.

Ghali, A., & Favre, R. (1994). *Concrete Structures, Stresses and Deformations* (2:nd ed.). London, United Kingdom of Great Britain and Northern Ireland: E & FN Spon.

Jönsson, G. (2010). *Fysik i Vätskor och Gaser* (8:th ed.). Lund, Sweden: Teach Support.

Kamali, A. Z., Johansson, M., & Svedholm, C. (2013). *Effects of restrained thermal strains in transversal direction of concrete slab frame brdiges.* Stockholm, Sweden: Royal Institute of Technology.

Kamrad, T. (2016, Januari 4). Experienced bridge designer. (R. Almén, Interviewer)

Ledin, J., & Christensson, O. (2015). *Cracking Assessment of Concrete Slab Frame Bridges Exposed to Thermally Induced Restraint Forces.* Stockholm, Sweden: Royal Institute of Technology.

SS 13 70 10. (2002). *Betongkonstruktioner - Täckande betongskikt.* Stockholm, Sweden: SIS Swedish Standard Institute.

SS-EN 1991-1-5. (2003). *Eurocode 1: Actions on structures - Part 1-5: General actions - Thermal actions.* Brussels, Belgium: CEN.

SS-EN 1992-1-1. (2005). *Eurocode 2: Design of concrete structures - Part 1-1: General Common rules for building and civil engineering structures.* Brussels, Belgium: CEN.

SS-EN 1992-2. (2005). *Eurocode 2: Design of concrete structures - Part 2: Concrete bridges - Design and detailing rules.* Brussels, Belgium: CEN.

Sundquist, H. (2009). *Infrastructure Structures* (2:nd ed.). Stockholm, Sweden: Royal Institute of Technology.

Sällfors, G. (2009). *Geoteknik* (4:th ed.). Gothenburg, Sweden: Chalmers.

The Concrete Society. (1992). *Non-structural cracks in concrete.* Wexham, United Kingdom of Great Britain and Northern Ireland: The Concrete Society.

TK Geo 11. (2011). *Trafikverkets tekniska krav för geokonstruktioner TK Geo 11.* Borlänge, Sweden: Swedish Transport Administration.

TRVFS 2011:12. (2011). *Trafikverkets författningssamling.* Borlänge, Sweden: Swedish Transport Administration.

TRVK Bro 11. (2011). *Trafikverkets tekniska krav Bro.* Borlänge, Sweden: Swedish Transport Administration.

TRVR Bro 11. (2011). *Trafikverkets tekniska råd Bro.* Borlänge, Sweden: Swedish Transport Administration.

Vägverket. (1993). *Vägverket BRO Handbok för broinspektion.* Borlänge, Sweden: Swedish Road Administration (now part of Swedish Transport Administration).

8. Appendix 1 – Results

Results for 12-404-1

Results for the right front wall are shown below.

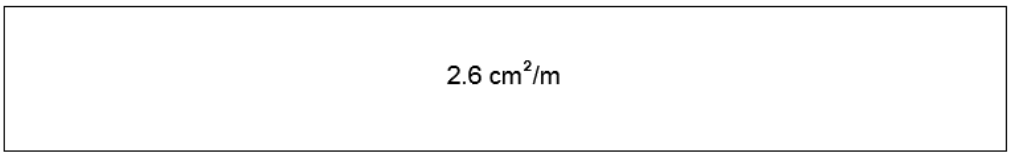

Figure 39 – Present reinforcement according to technical drawing.

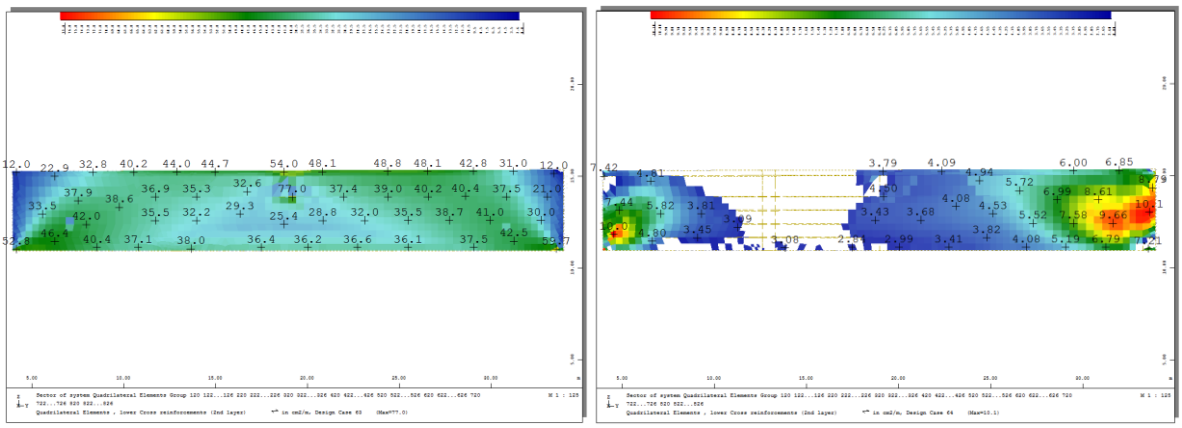

Figure 40 – Reinforcement need for the front walls. Results 2.6 cm²/m are cut out.

Results for the valve are shown below.

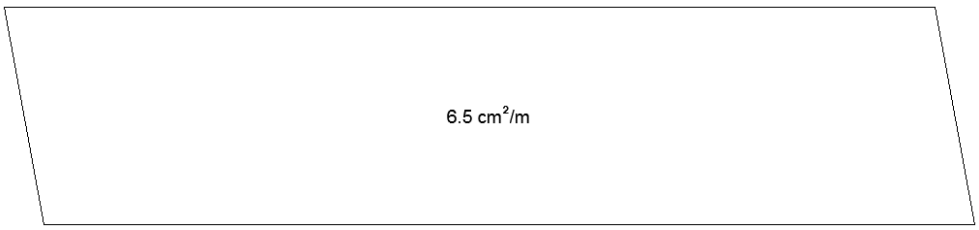

Figure 41 – Present reinforcement according to technical drawing.

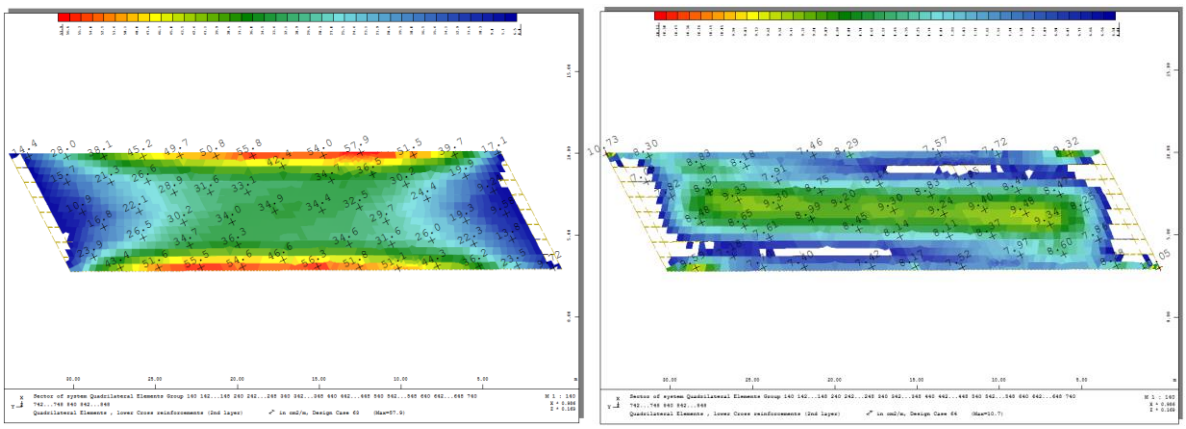

Figure 42 – Skewed reinforcement need for the valve. Results below 6.5 cm²/m are cut out.

Observations in the field yielded the following results:

- Observation showed that both the front walls and the valve were cast in five phases.
- A single crack was found in all but one cast phases with widths varying between 0.1 and 0.2 mm. Furthermore one of the cracks had a diagonal shape, see Figure 51.
- Two large longitudinal cracks were discovered at either side of the bridge. Furthermore a small transversal crack was also discovered, see Figure 52.

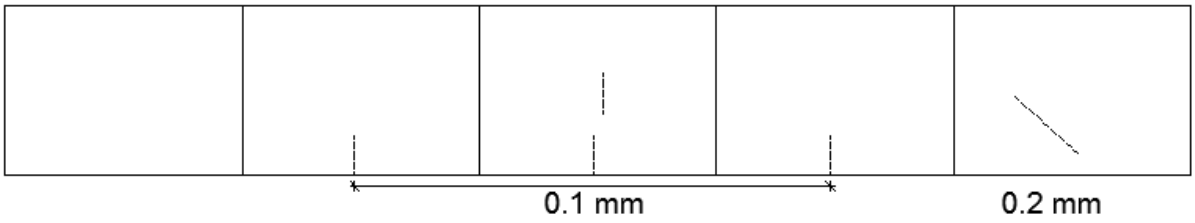

Figure 43 - Observed cracks in the front wall.

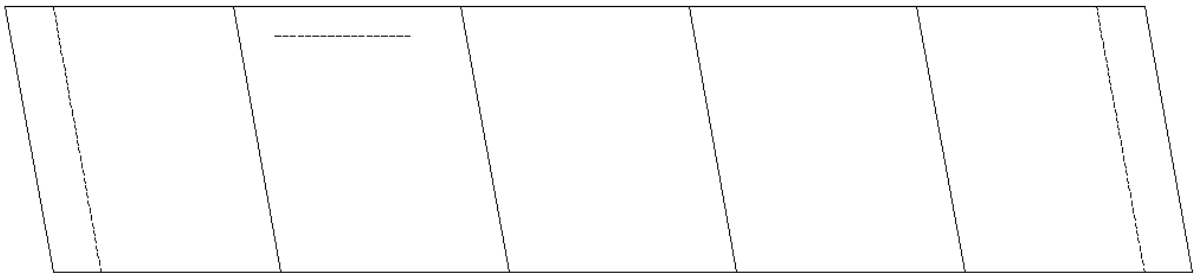

Figure 44 - Observed cracks in the valve

Results for 12-438-1

Results for the right front wall are shown below.

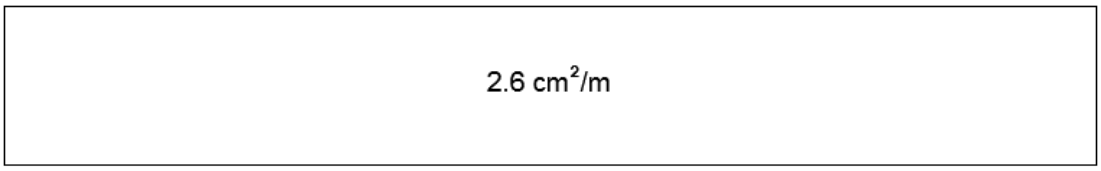

Figure 45 – Present reinforcement according to technical drawing.

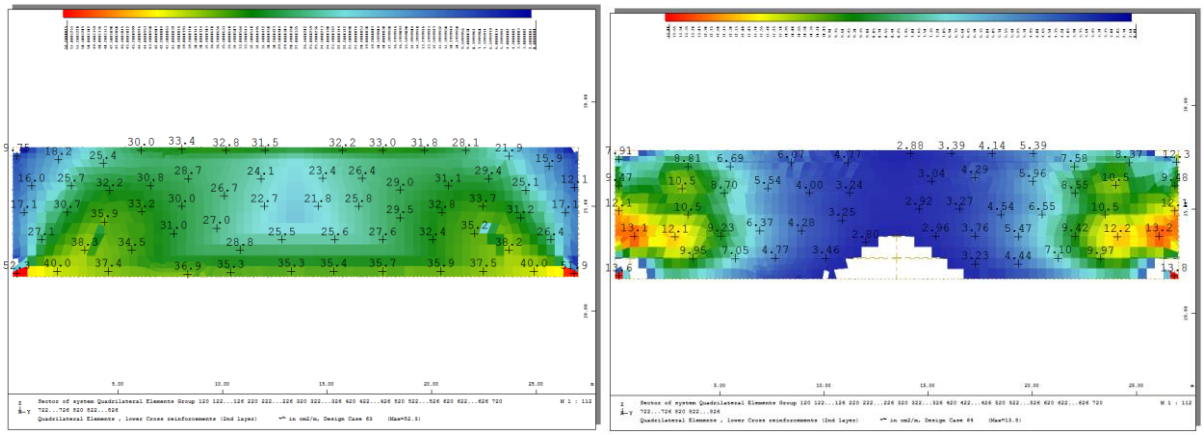

Figure 46 – Reinforcement need for the front walls. Results below 2.6 cm²/m are cut out.

Results for the valve are shown below.

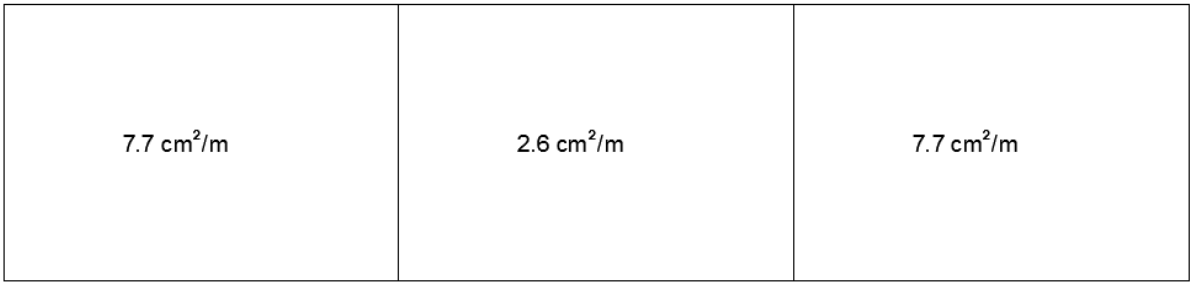

Figure 47 – Present reinforcement according to technical drawing.

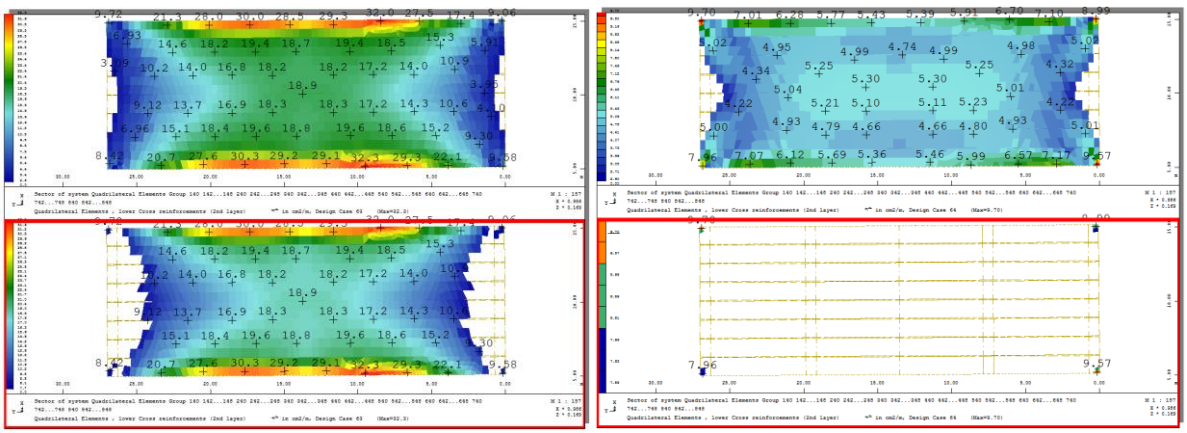

Figure 48 – Orthogonal reinforcement need for the valve. Results below 2.6 and 7.7 cm²/m are cut out.

Observations in the field yielded the following results:

- Observation showed that both the front walls were cast in four phases and the valve was cast in three phases. There were also hints of repairs and injections in the front walls.
- A small number of both longitudinal and transversal cracks with a width of 0.1 m were found spread out in all cast phases, see Figure 57.
- No cracks were discovered in the valve.

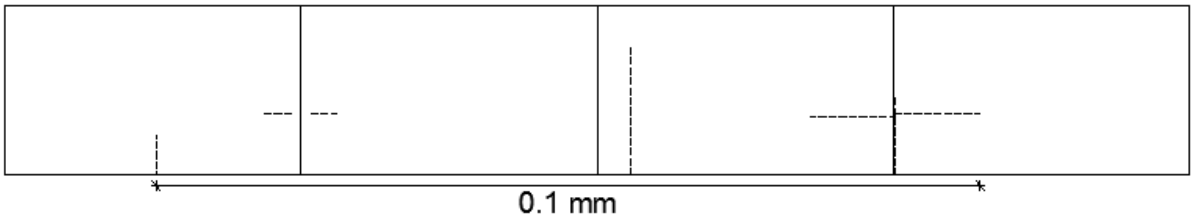

Figure 49 - Observed cracks in the front wall.

Results for 12-598-1

Results for the right front wall are shown below.

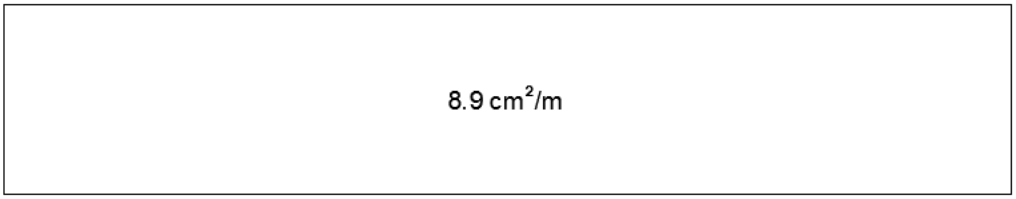

Figure 50 – Present reinforcement according to technical drawing.

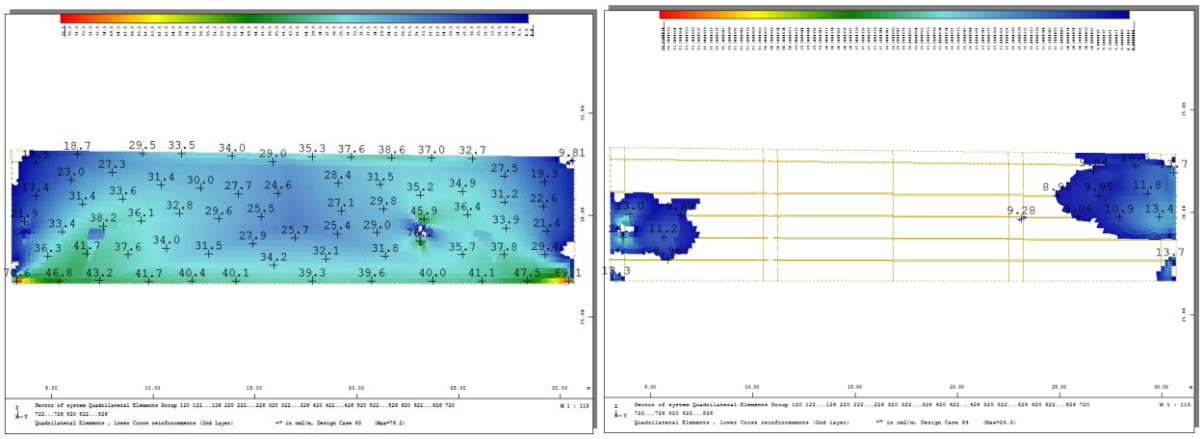

Figure 51 – Reinforcement need for the front walls. Results below 8.9 cm²/m are cut out.

Results for the valve are shown below.

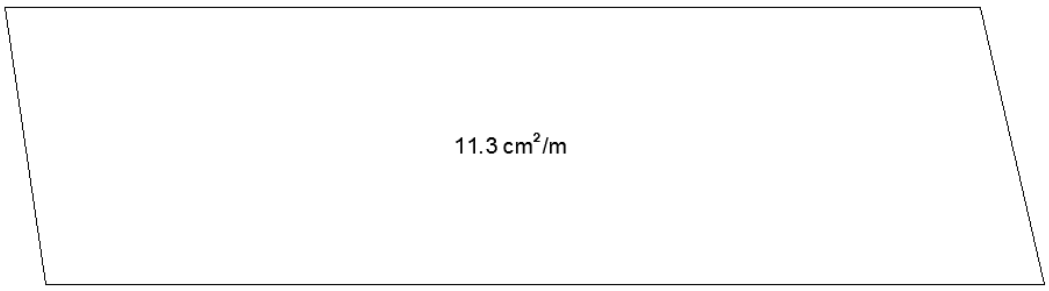

Figure 52 – Present reinforcement according to technical drawing.

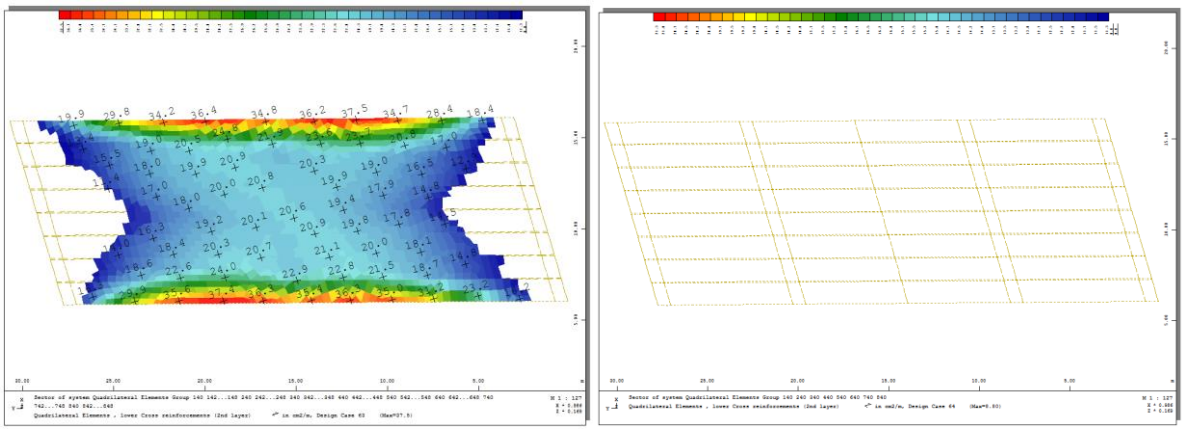

Figure 53 – Skewed reinforcement need for the valve. Results below 11.3 cm²/m are cut out.

Observations in the field yielded the following results:

- Observation showed that both the front walls were cast in 4 phases and the valve was cast in three phases. Additionally hints of repairs and injections were found in the front walls.
- A small number of cracks between 0.1 and 0.2 mm were found in all but one cast phases, see Figure 62.
- A small longitudinal crack was found in the middle of the valve, see Figure 63.

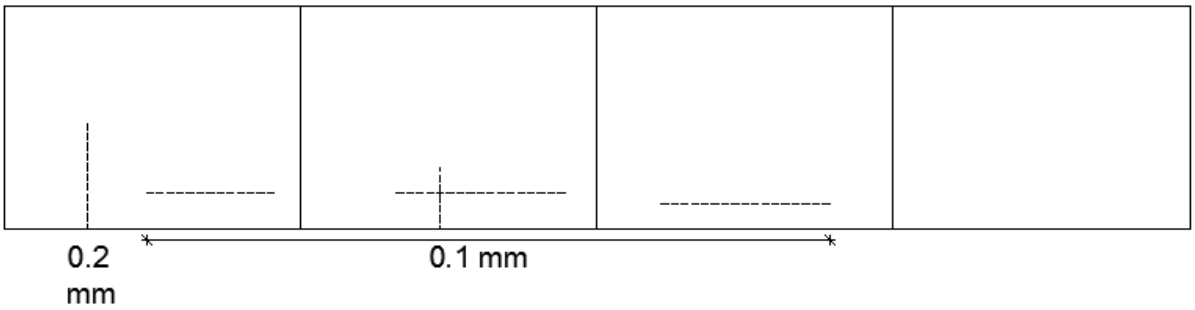

Figure 54 - Observed cracks in the front wall.

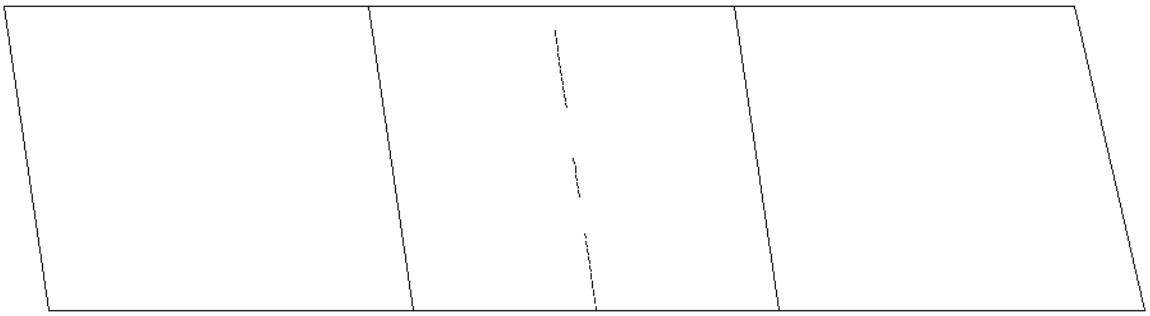

Figure 55 - Observed cracks in the valve

Results for 12-605-1

Results for the right front wall are shown below.

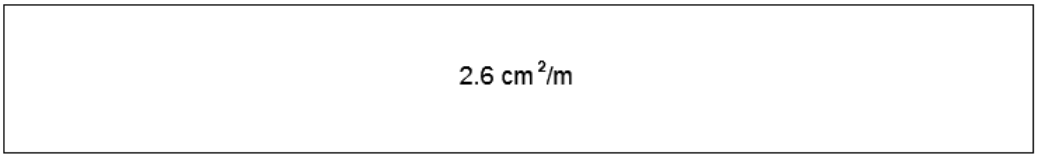

Figure 56 – Present reinforcement according to technical drawing.

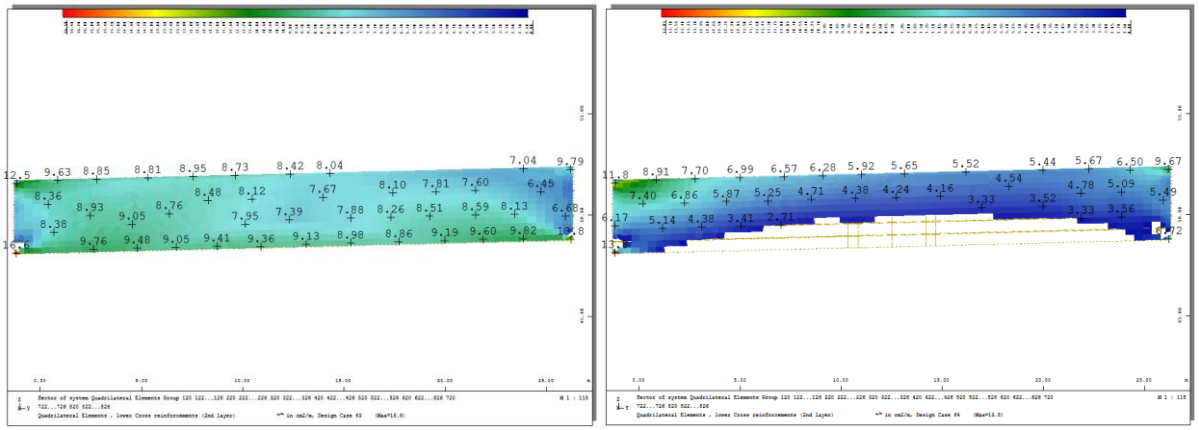

Figure 57 – Reinforcement need for the front walls. Results below 2.6 cm²/m are cut out.

Results for the valve are shown below.

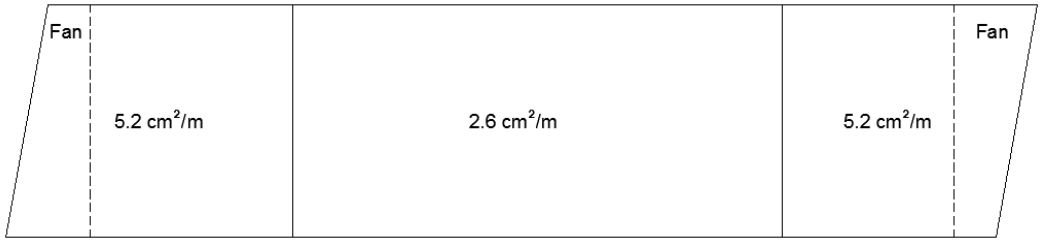

Figure 58 – Present reinforcement according to technical drawing.

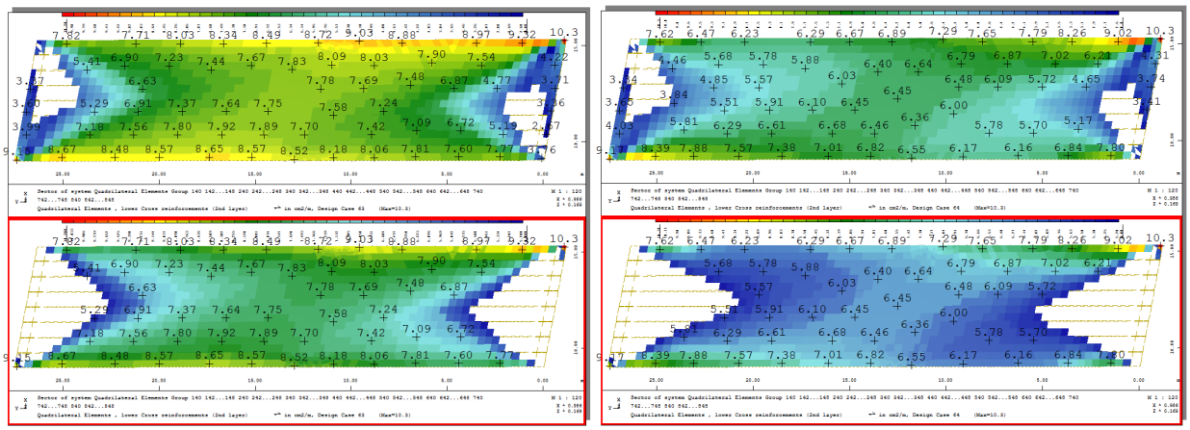

Figure 59 – Orthogonal reinforcement need for the valve. Results below 2.6 and 5.2 cm²/m are cut out.

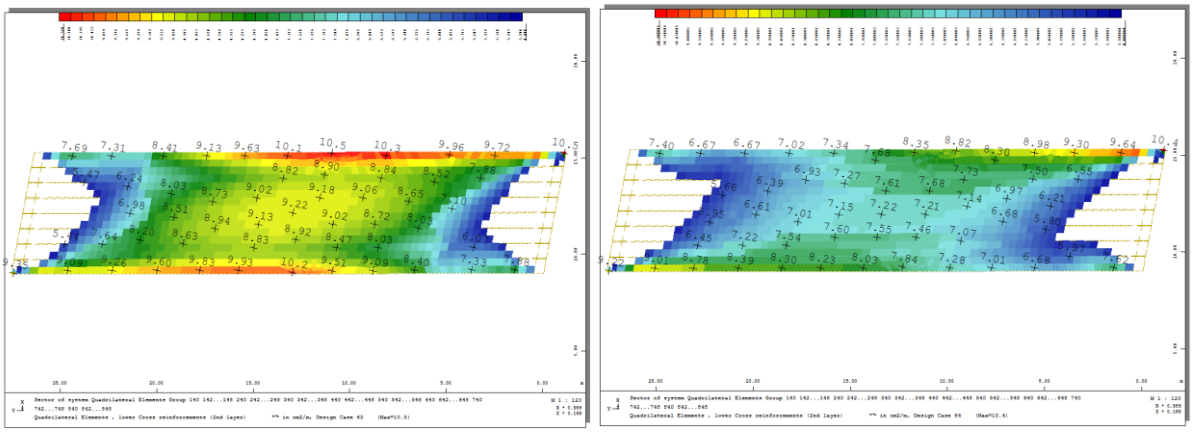

Figure 60 – Skewed reinforcement need for the valve. Results below 5.2 cm^2/m are cut out.

Observations in the field yielded the following results:

- Observation showed that both the front wall and the valve were cast in three phases with two expansion joints.
- A handful of cracks between 0.1 and 0.3 mm were found in all cast phases. Furthermore a huge crack was found in the middle of the front wall with a width of 2.0 mm, see Figure 69.
- A large sprawling longitudinal crack was found in the middle of the valve which was connected to the huge crack in the front wall, see Figure 70.

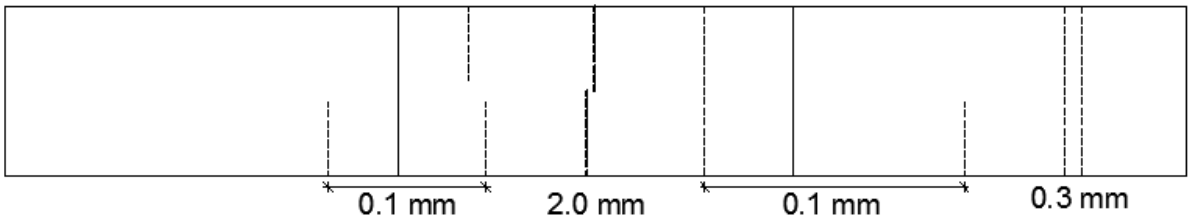

Figure 61 - Observed cracks in the front wall.

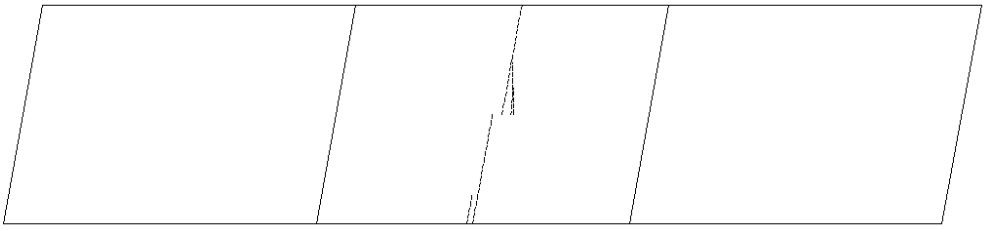

Figure 62 - Observed cracks in the valve

Results for 12-606-1

Results for the right front wall are shown below.

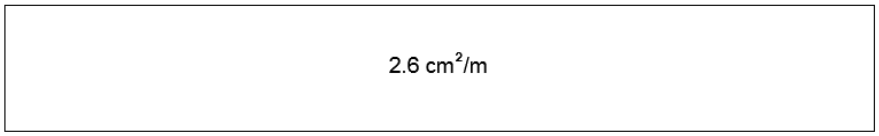

Figure 63 – Present reinforcement according to technical drawing.

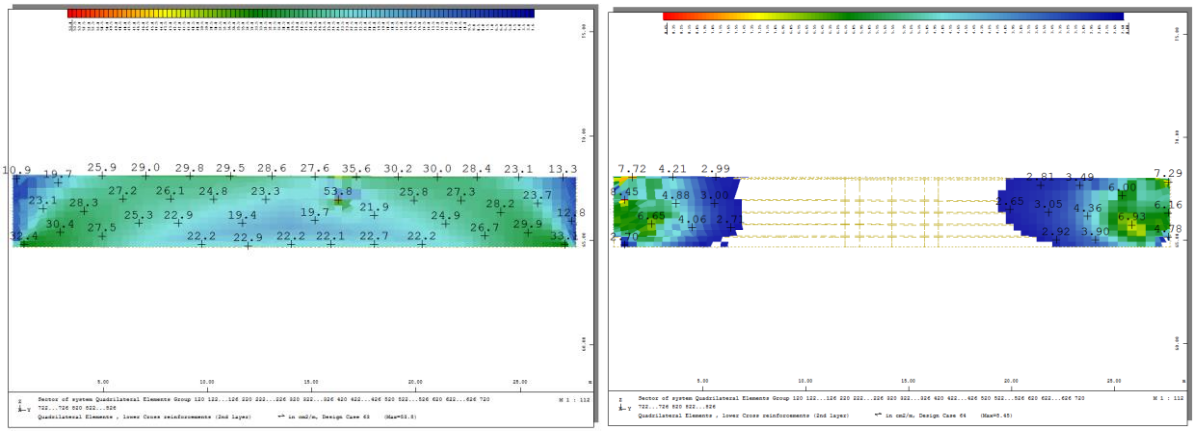

Figure 64 – Reinforcement need for the front walls. Results below 2.6 cm²/m are cut out.

Results for the valve are shown below.

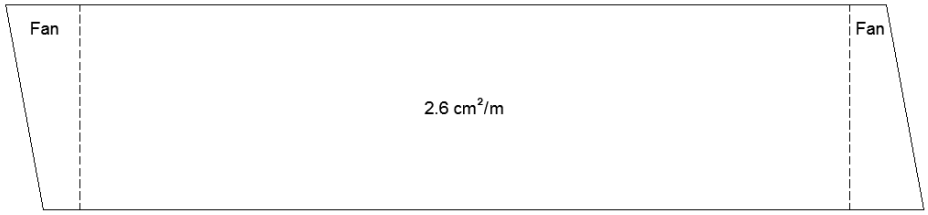

Figure 65 – Present reinforcement according to technical drawing.

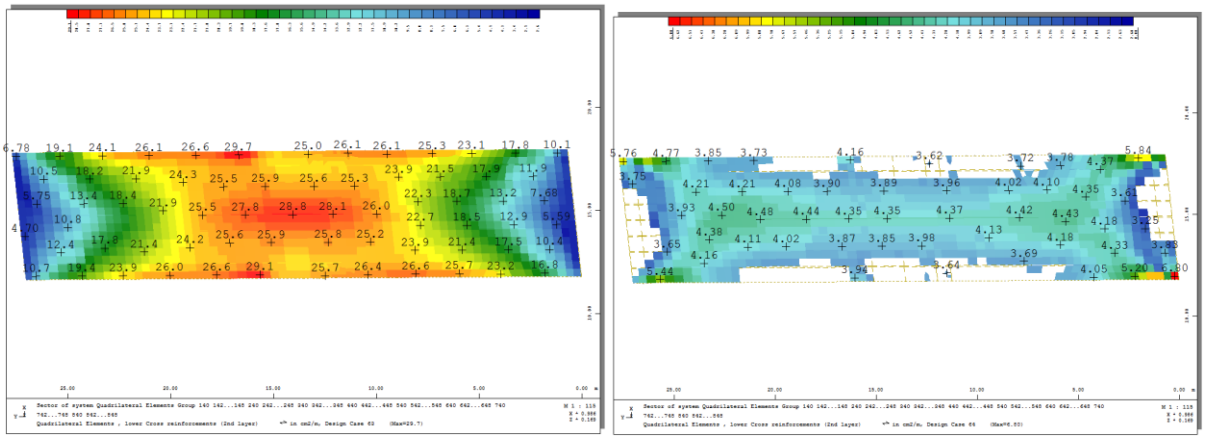

Figure 66 - Orthogonal reinforcement need for the valve. Results below 2.6 are cut out.

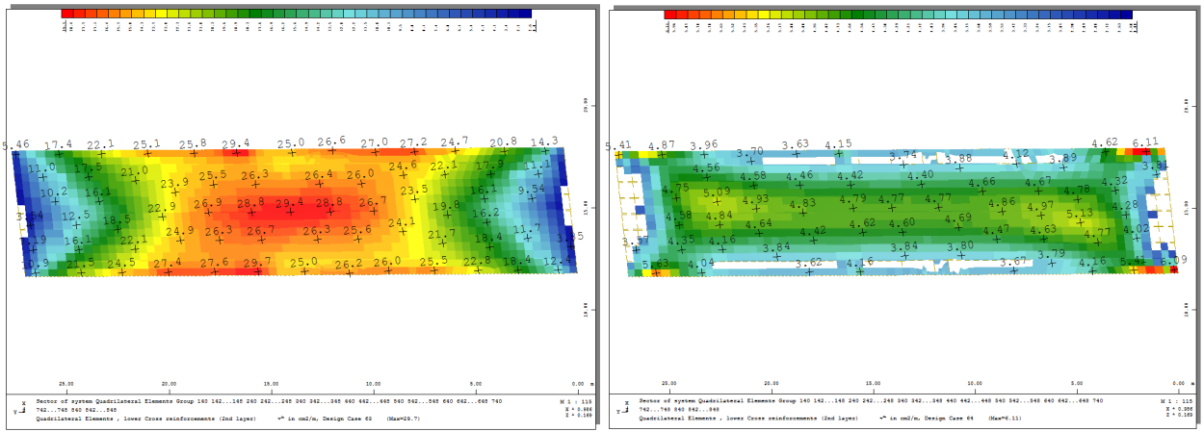

Figure 67 - Skewed reinforcement need for the valve. Results below 2.6 are cut out.

Observations in the field yielded the following results:

- The interior of the tunnel was heavily painted so it was hard to both detect cracks as well as to decide the crack width. Observation also showed that both the front wall and the valve were cast in three phases, with two expansion joints.
- Multiply cracks between 0.1 and 0.2 mm were found in all cast phases, see Figure 76.
- Three sprawling longitudinal crack was found in the middle of the valve's cast phases, see Figure 77.

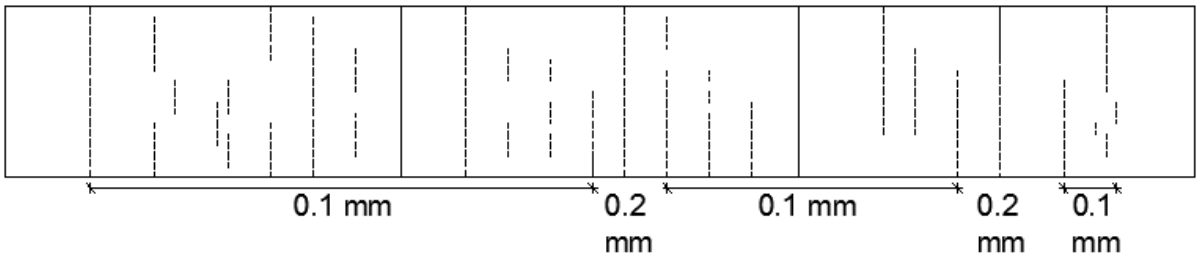

Figure 68 - Observed cracks in the front wall.

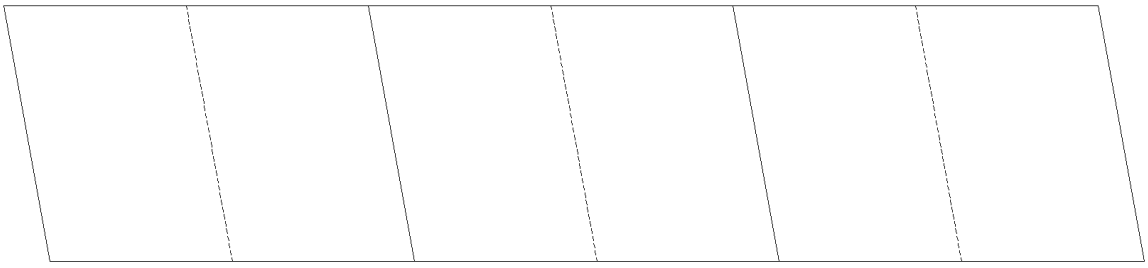

Figure 69 - Observed cracks in the valve.

Results for 12-650-1

Results for the right front wall are shown below.

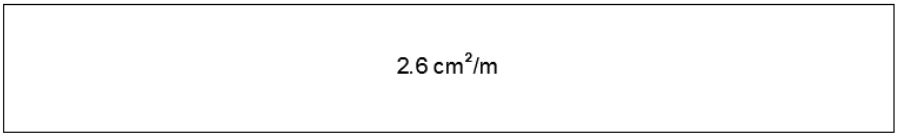

Figure 70 – Present reinforcement according to technical drawing.

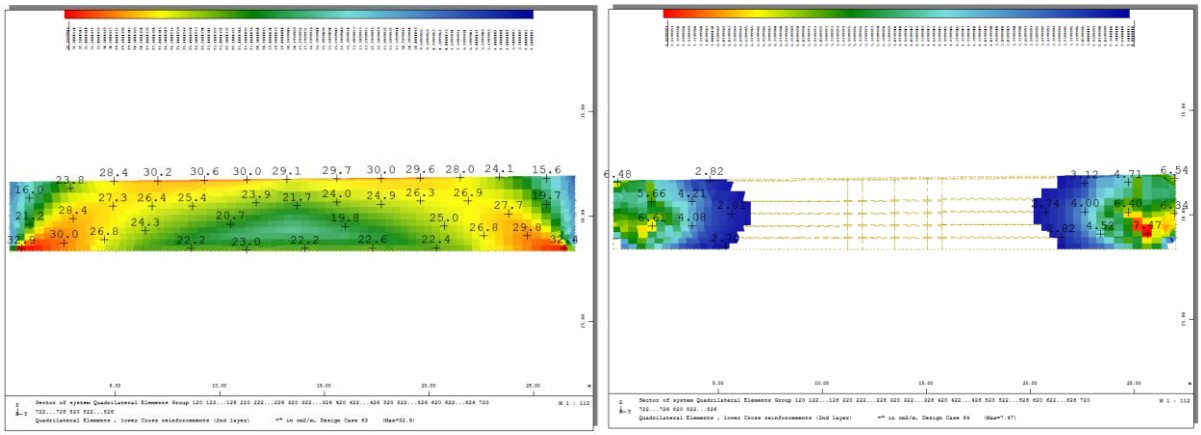

Figure Reinforcement need for the front walls. Results below 2.6 cm²/m are cut out.

Results for the valve are shown below.

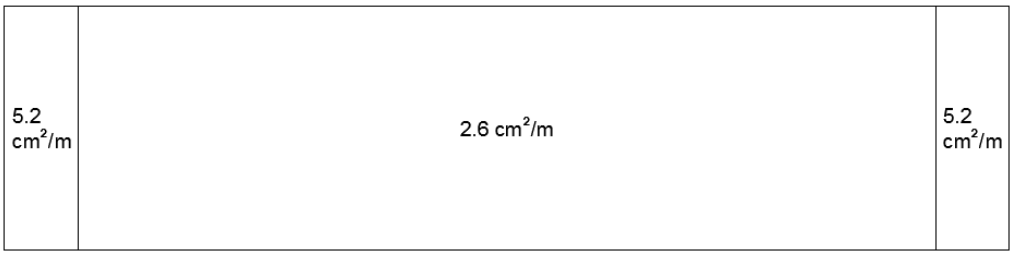

Figure 71 – Present reinforcement according to technical drawing.

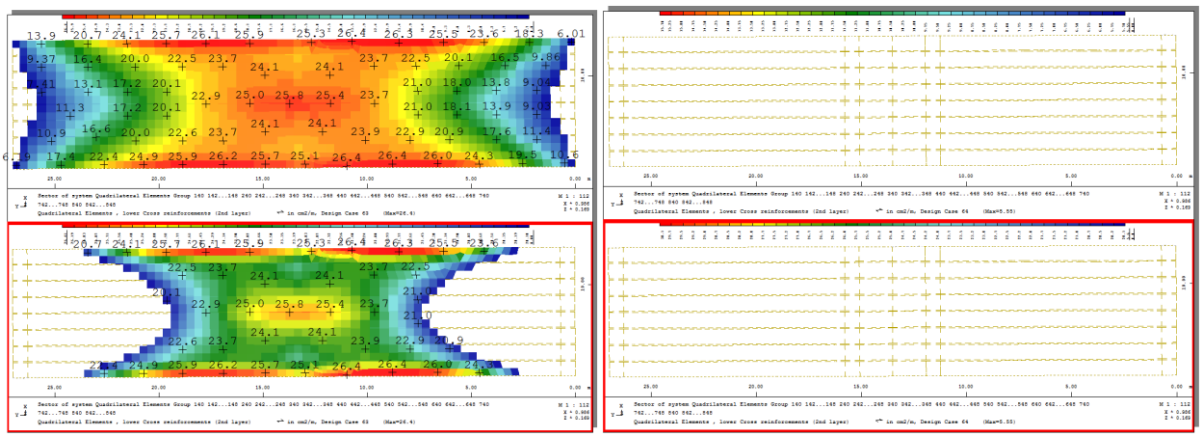

Figure 72 - Reinforcement need for the valve. Results below 2.6 and 5.2 cm²/m are cut out.

Observations in the field yielded the following results:

- The interior of the tunnel was heavily painted so it was hard to both detect cracks as well as to decide the crack width. Observation also showed that both the front wall and the valve were cast in three phases, with two expansion joints.
- Only a few cracks between 0.1 and 0.2 mm were found spread out in all cast phases on the frame walls, see Figure 81.
- Only hints of longitudinal cracks between the light fixtures and frame wall were found in the valve, see Figure 82.

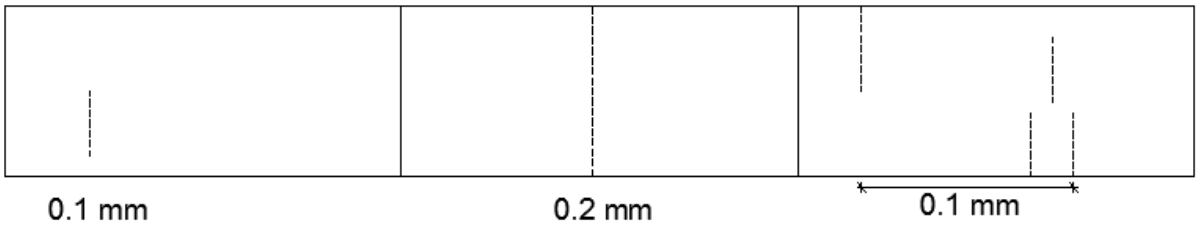

Figure 73 - Observed cracks in the front wall.

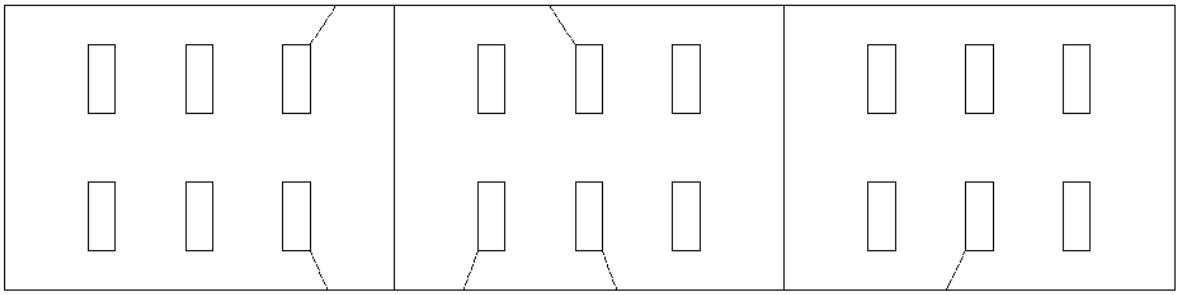

Figure 74 - Observed cracks in the valve.

Results for 12-921-1

Results for the right front wall are shown below.

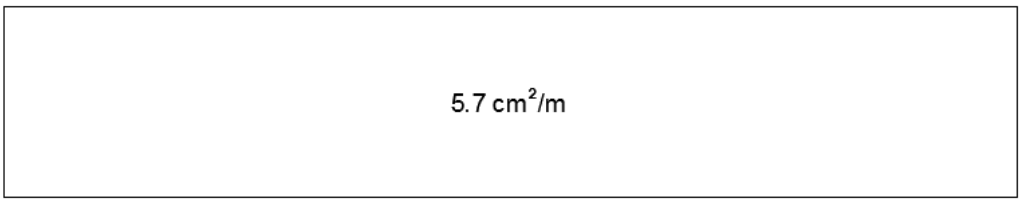

Figure 75 – Present reinforcement according to technical drawing.

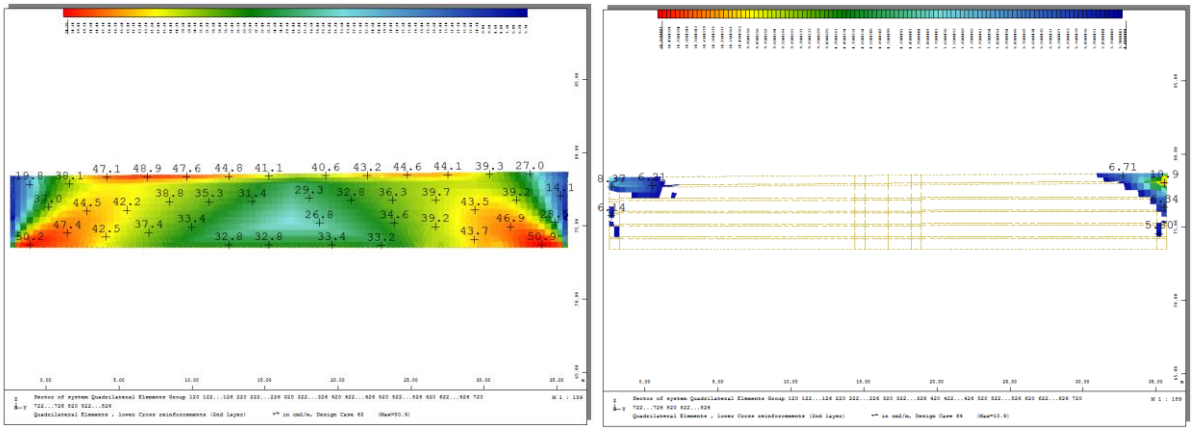

Figure 76 – Reinforcement need for the front walls. Results below 5.7 cm²/m are cut out.

Results for the valve are shown below.

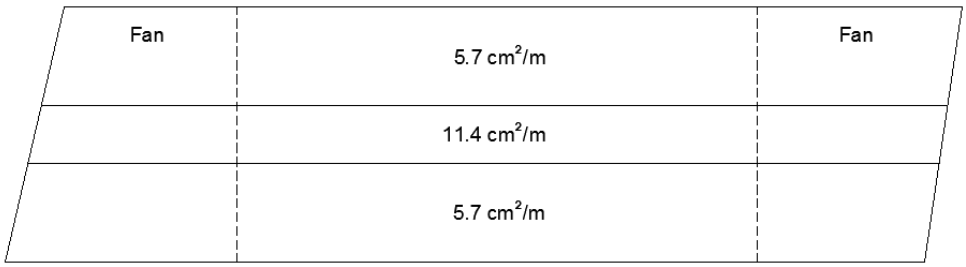

Figure 77 – Present reinforcement according to technical drawing.

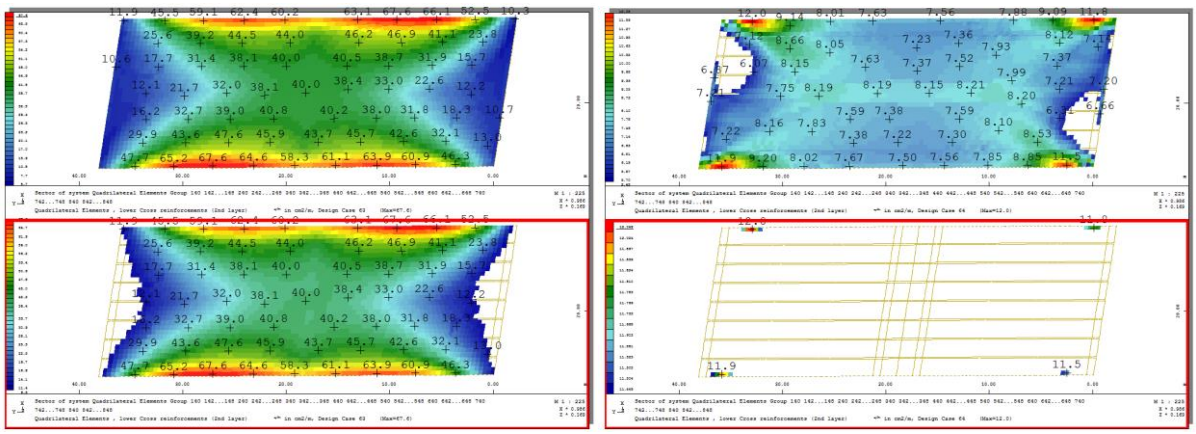

Figure 78 – Orthogonal reinforcement need for the valve. Results below 5.7 and 11.4 cm²/m are cut out.

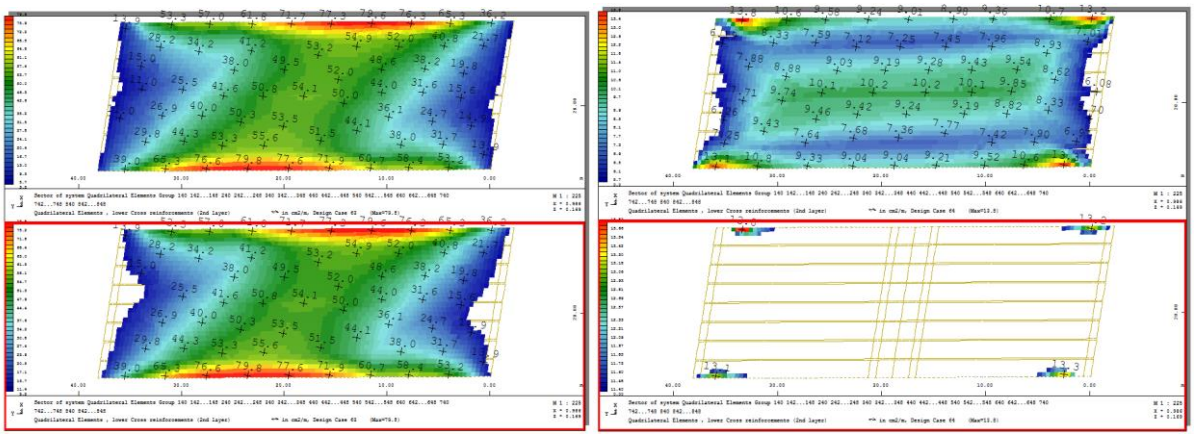

Figure 79 - Skewed reinforcement need for the valve. Results below 5.7 and 11.4 cm^2/m are cut out.

Observations in the field yielded the following results:

- Observation also showed that both the front wall was cast in 8 phases and the valve was cast in three phases.
- A single crack was found in the middle of every cast phase of the front wall. Additionally a crack was also found on one of the joints on the front wall, see Figure 88.
- No cracks were found on the valve.

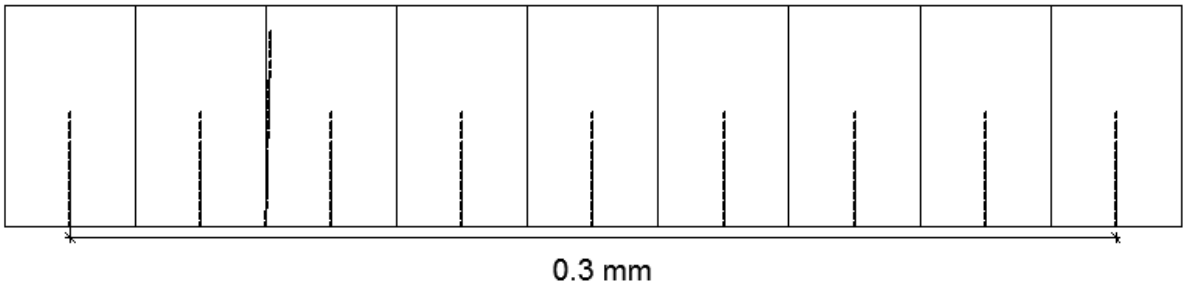

Figure 80 - Observed cracks in the front wall.

Results for 12-926-1

Results for the right front wall are shown below.

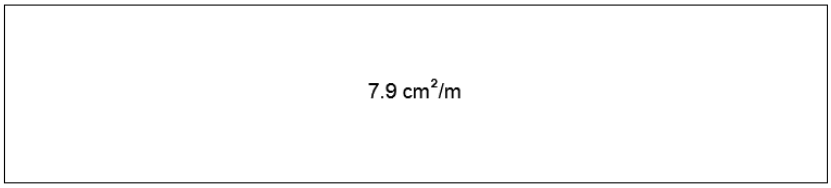

Figure 81 – Present reinforcement according to technical drawing.

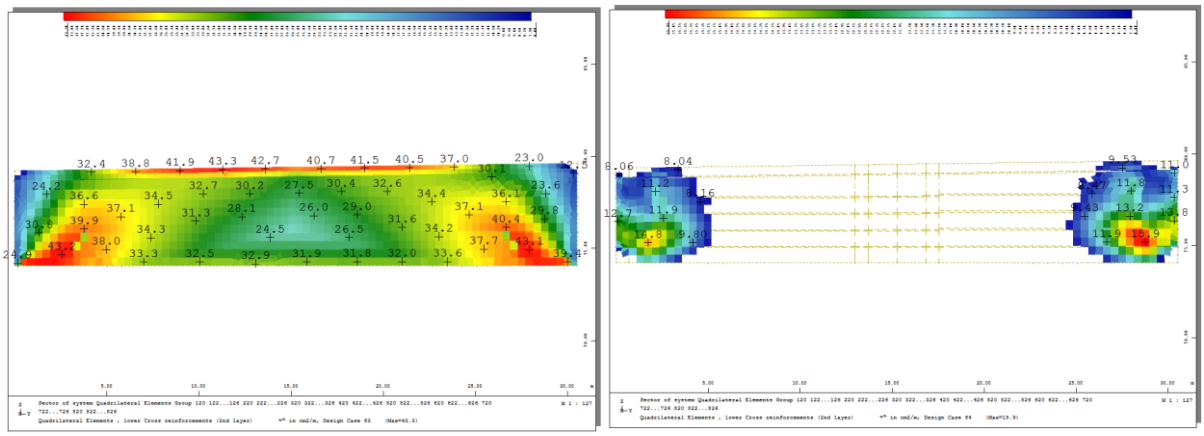

Figure 82 – Reinforcement need for the front walls. Results below 7.9 cm²/m are cut out.

Results for the valve are shown below.

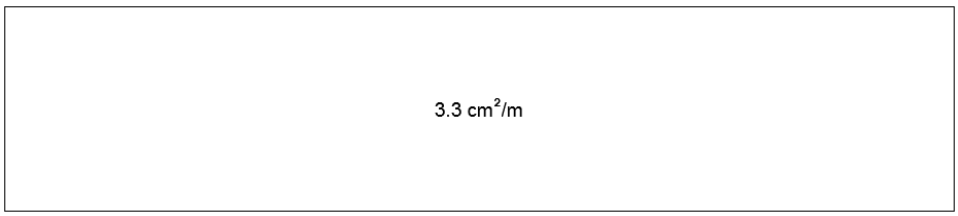

Figure 83 – Present reinforcement according to technical drawing.

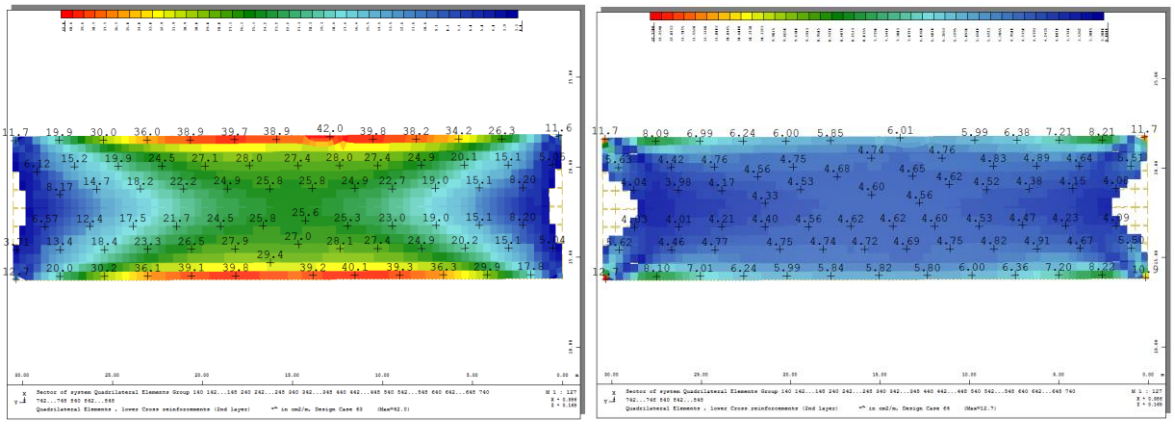

Figure 84 - Reinforcement need for the valve. Results below 3.3 cm²/m are cut out.

Observations in the field yielded the following results:

- Observation showed that both the front walls and the valve were cast in three phases where with two larger and one smaller block.
- A small number of cracks between 0.1 and 0.3 mm were found in the two larger cast phases, see Figure 93.
- No cracks in the valve were found.

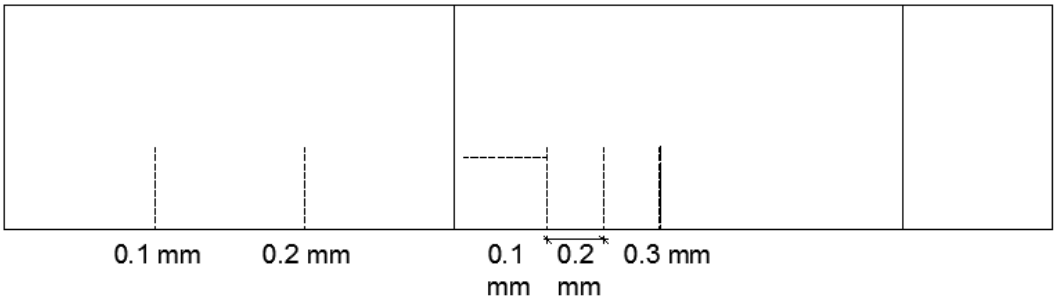

Figure 85 - Observed cracks in the front wall.

Results for 12-927-1

Results for the right front wall are shown below.

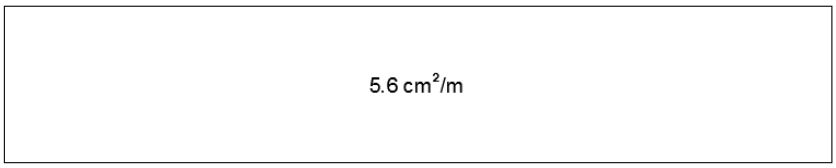

Figure 86 – Present reinforcement according to technical drawing.

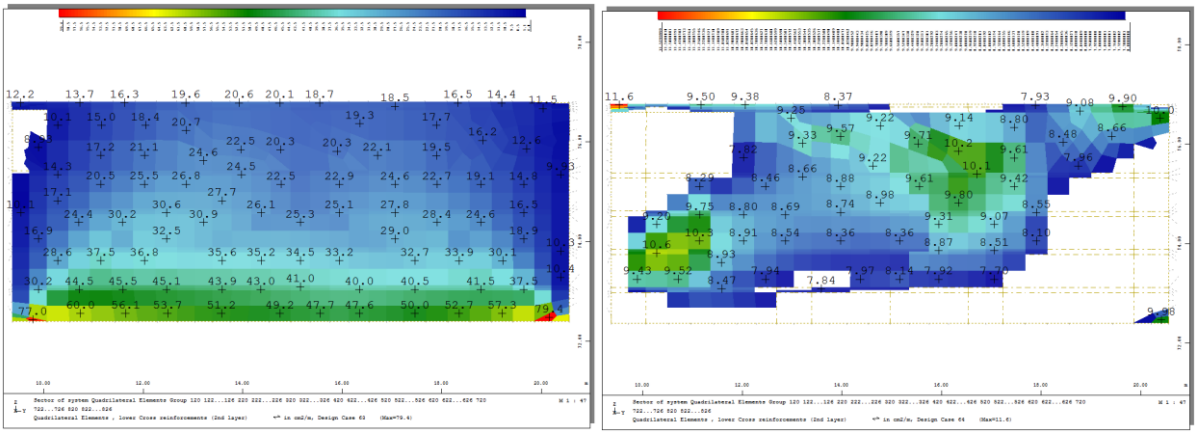

Figure 87 – Above: <5.7 cm²/m cut out. Below: <15.7 cm²/m cut out.

Results for the valve are shown below.

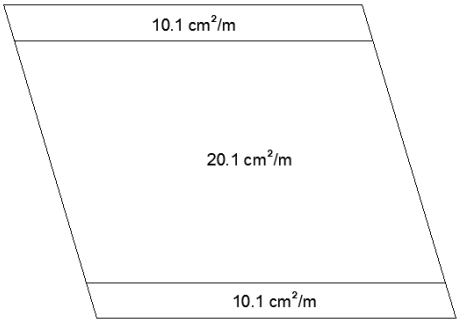

Figure 88 – Present reinforcement according to technical drawing.

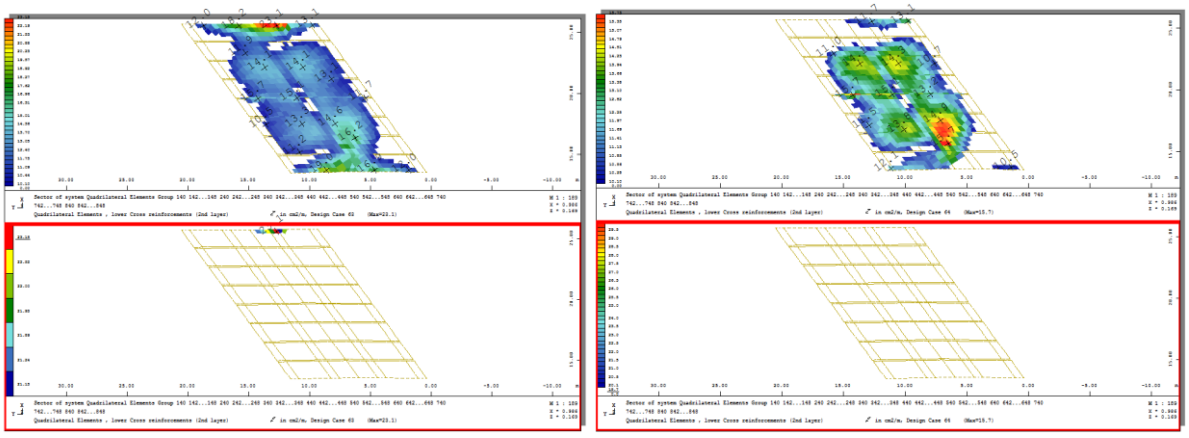

Figure 89 – Skewed reinforcement need for the valve. Results below 3.3 cm²/m are cut out.

Observations in the field yielded no results since access to the bridge was denied due to its location within the construction area of the European Spallation Source.

9. Appendix 2 – Photos

Figure 90 - Cracks in bridge 12-404-1. Left is front wall and right is valve.

Figure 91 - Cracks in bridge 12-438-1. Left is front wall and right is construction join for front wall.

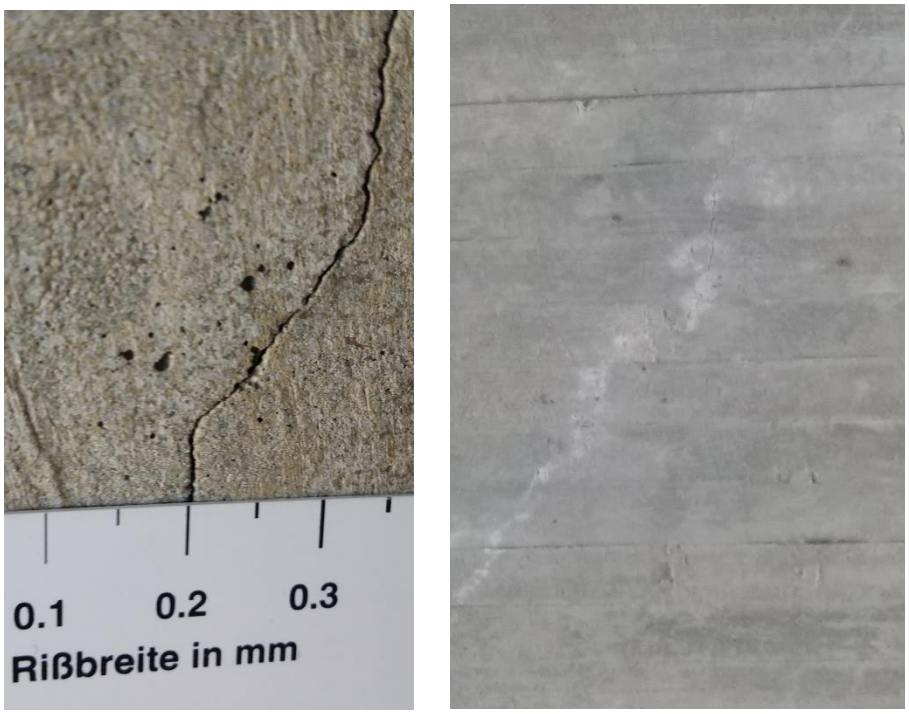

Figure 92 - Cracks in bridge 12-598-1. Left is front wall and right is valve.

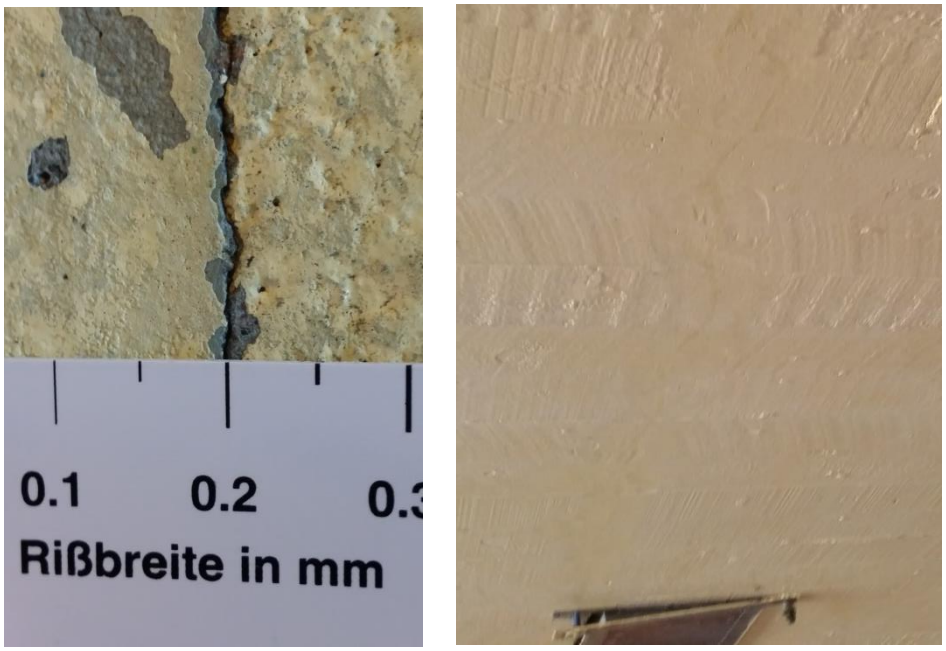

Figure 93 - Cracks in bridge 12-604-1. Left is front wall and right is valve.

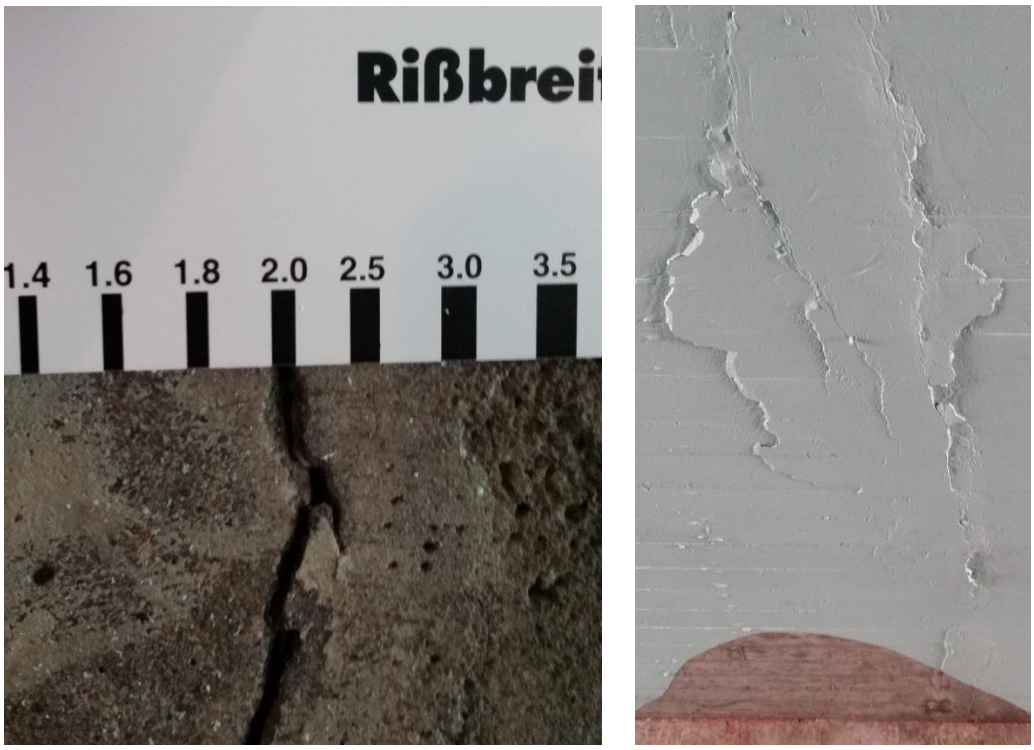

Figure 94 - Cracks in bridge 12-605-1. Left is front wall and right is valve.

Figure 95 – Cracks in bridge 12-606-1. Left is front wall and right is valve.

Figure 96 - Cracks in bridge 12-650-1. Left is front wall and right is valve.

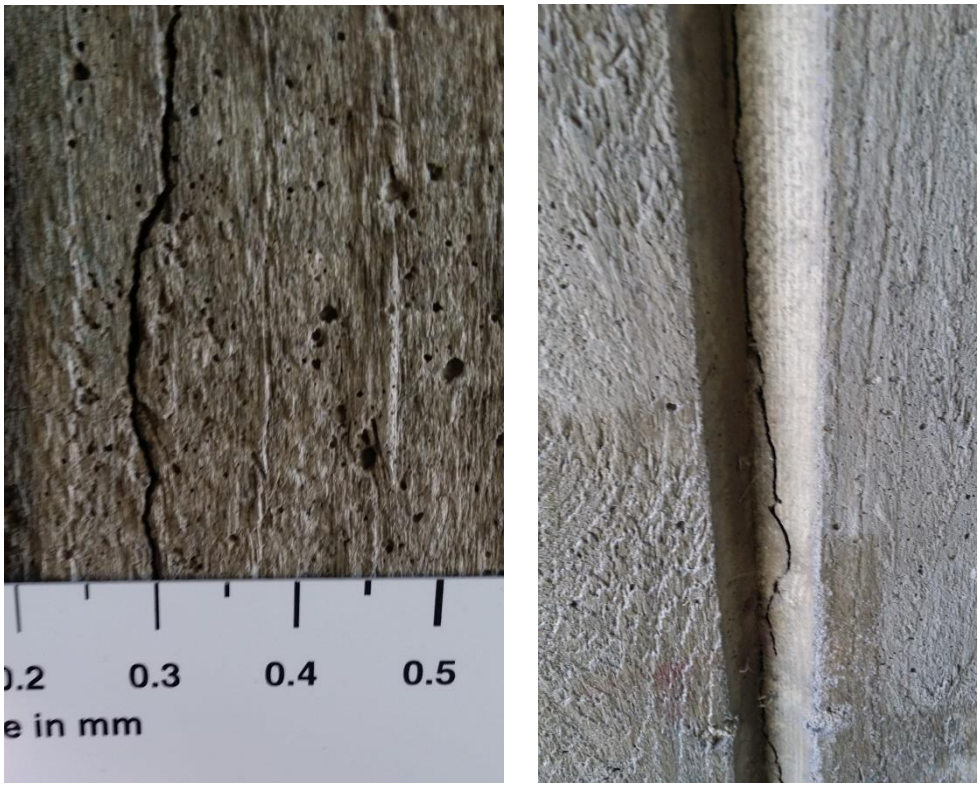

Figure 97- Cracks in bridge 12-921-1. Left is front wall and right is construction joint for front wall.

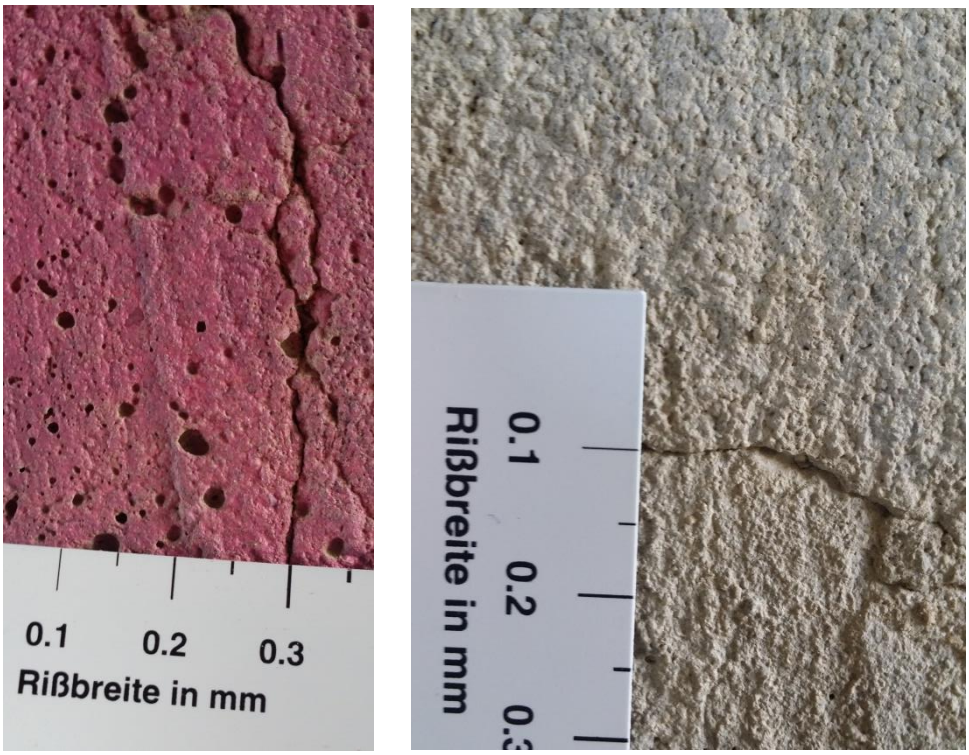

Figure 98 - Cracks in bridge 12-926-1. Left is in front wall and right is transversal crack in front wall.

Figure 99 – Crack in bridge 12-1374-1. Only a single crack in the construction join for the valve was found.

10. Appendix 3 – Technical drawings

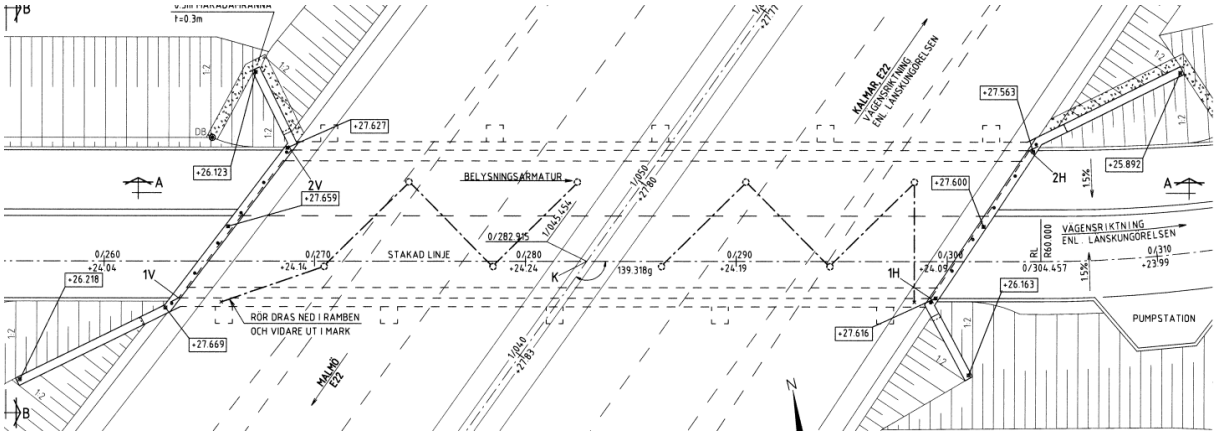

11. Figure 100 – Plane drawing for bridge 12-1374-1.

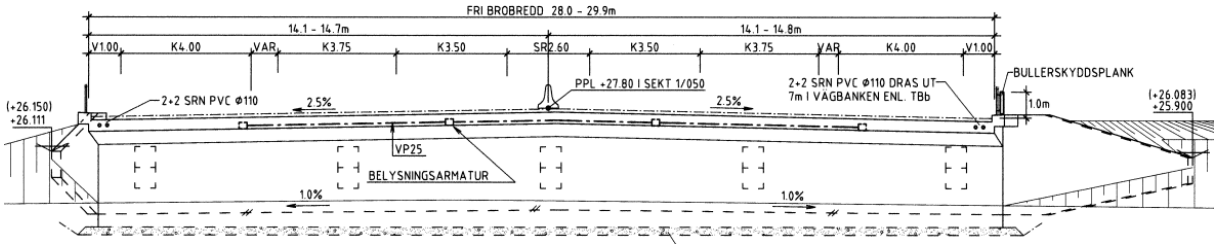

12. Figure 101 – Elevation drawing for bridge 12-1374-1.

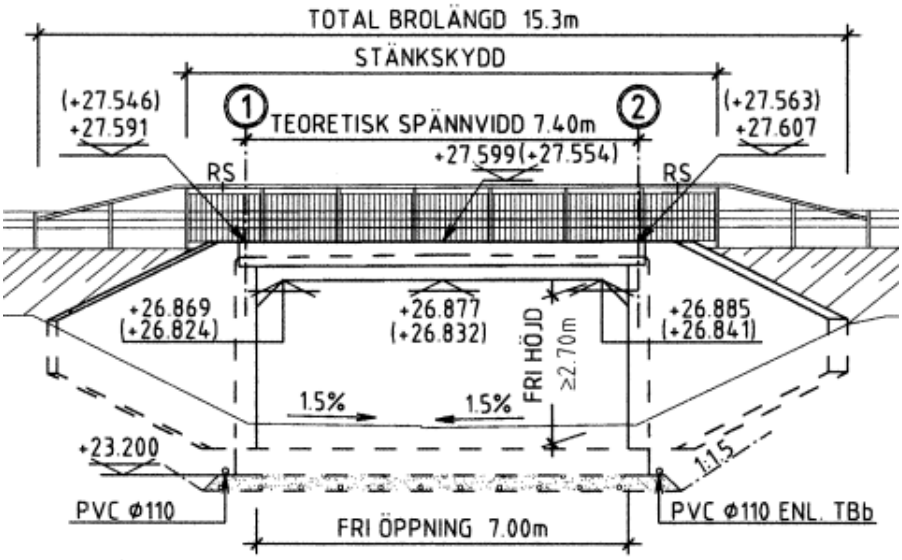

13. Figure 102 – Section drawing for bridge 12-1374-1.

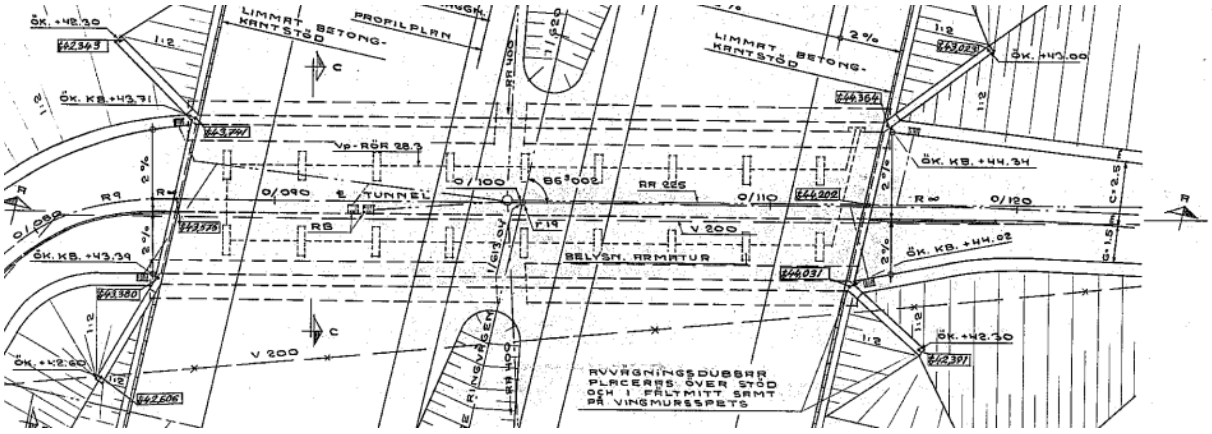

Figure 103 – Plane drawing for bridge 12-604-1.

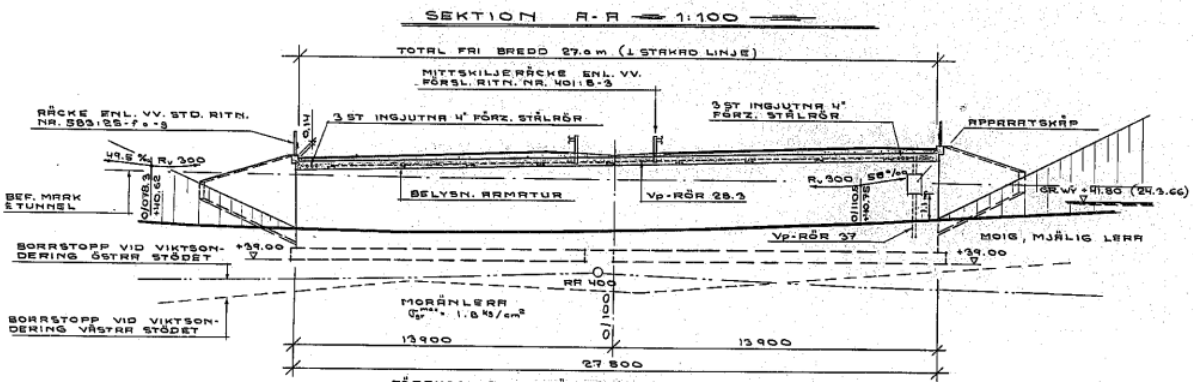

Figure 104 – Elevation drawing for bridge 12-604-1.

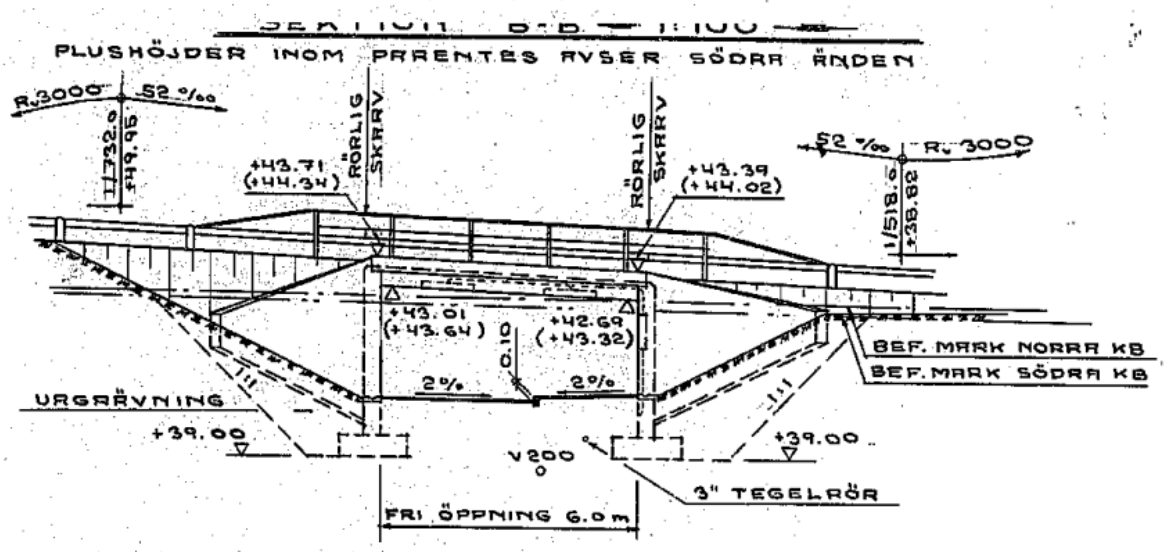

Figure 105 – Section drawing for bridge 12-604-1.